Remote sensing based flood modelling; Morales Island, Magdalena River floodplain, Colombia.

ROBERTO JARAMILLO VASQUEZ
February, 2016

SUPERVISORS:
Prof. Dr. V.G. JETTEN (Victor)
Dr. Ing. T.H.M. RIENTJES (Tom)

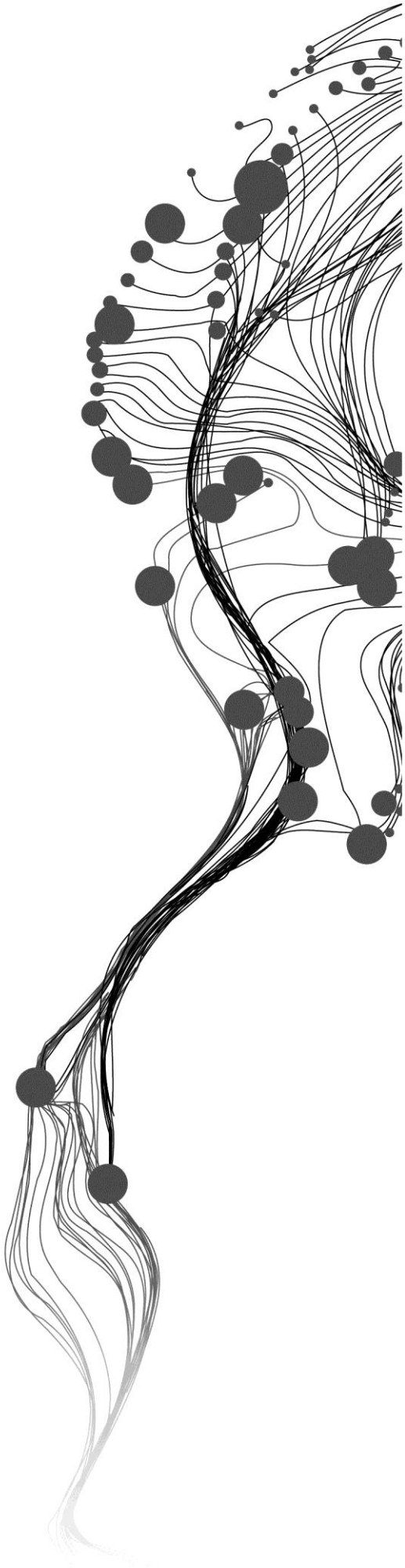

Remote sensing based flood modelling; Morales Island, Magdalena River floodplain, Colombia.

ROBERTO JARAMILLO VASQUEZ
Enschede, The Netherlands, February, 2016

Thesis submitted to the Faculty of Geo-Information Science and Earth Observation of the University of Twente in partial fulfilment of the requirements for the degree of Master of Science in Geo-information Science and Earth Observation for:
Applied Earth Sciences with Specialization in Natural Hazards, Risk and Engineering.

SUPERVISORS:
Prof. Dr. V.G. JETTEN (Victor)
Dr. Ing. T.H.M. RIENTJES (Tom)

THESIS ASSESSMENT BOARD:
Dr. N. Kerle (Norman) - Chair
Dr. R. van Beek (Rens) External Examiner, Utrecht University

ABSTRACT

For a study area in the Magdalena River floodplain in Colombia, this research describes the use of remote sensing to overcome data scarcity when applying and evaluating hydrodynamic modelling. For reliable performance flood models require accurate data; lacking detail on boundary conditions, terrain and river geometry, has determinant effect on the simulations. No measure of flood is available for the study area so remote sensing based flood extent maps were produced from Landsat as validation sets of observed floods. To parameterize surface roughness, land cover maps were produced from Landsat. Furthermore the terrain elevation was based on the CGIAR SRTM DEM. In absence of cross section measurements combined use of cover and elevation data aided to represent the river network and dimensions. IDEAM stage and discharge daily series were to calculate return periods for high river flows, which ranged between 4.4-17.5 on the upstream boundary. With this list of high flows & dates, close scenes were searched in Landsat and MODIS data for flood evidences and date selection for 1D2D simulations. 1D2D SOBEK model was set up, where simulation and evaluation of flood extents is the core of the study. Observed river flow was used as a base to calibrate model cross sections. Measurements in several stations along the river showed one day lag between a peak detected upstream and downstream, which was used to parameterize channel friction. The simulated river flow compared at two IDEAM river gauges gives a preliminary satisfactory results being able to partially reproduce the observed hydrograph in lower flows. Still overbank locations are not completely correct. Only the main river and channels are included in the current schematization, while water bodies and interconnections are not represented. Two other important discharge inflow measurements are also missing, preventing a correct definition of the upstream boundary condition. To analyse the effect of changing roughness, boundary conditions and resolution on simulated floods, resulting extents were contrasted on a pixel level to locate and quantify their difference. Contrast between the two largest observed flood extents was done, coinciding in 65%. Contrast between observed and simulated flood extents gave similarities in 65% for the case of 2011 and 30% for 2005. Resulting similar maximum extents prove the potential the model has to predict flooding in the study area. Flood simulations also reproduce correctly blocked and present water flow paths observed in satellite imagery. The grid with 90x90 meter resolution gives a more realistic representation of the simulated boundaries, and even though elevations on the 270x270 meter/pixel resolution gets averaged, it can in reproduce some flooding patterns and maximum extents. Channel overtopping drastically reduces the peak downstream. The model in construction is not able to reproduce correctly the receding water bodies observed with the satellite imagery, mainly due to the embankment set up and not including the internal drainage network of the river floodplain. The general assessment reveals quality issues in the model input data, not allowing optimal performance of the hydrodynamic model, rather orienting where to concentrate efforts in field measurements and monitoring to improve it. Computing capacity was limited and only allowed few simulations on 270x270 meter/pixel resolution which took around 5 hours to complete 3 months at daily time step. One single simulation on 90x90 meters/pixel resolution was carried out, for the same time period calculation time was 5 days.

Keywords: Floodplain, extreme events, high flows, flood extent, hydrodynamic flood modelling, 1D2D SOBEK model, Landsat, CGIAR SRTM DEM, remote sensing & GIS.

TABLE OF CONTENTS

LIST OF FIGURES

LIST OF TABLES

1. INTRODUCTION

1.1. Background

The Merriam Webster dictionary defines floodplain as "an area of low, flat land along a stream or river that may flood". The Nature Conservancy TNC defines them as "relatively flat areas that border a river and are prone to flooding". Floodplains are formed by the historic and present water dynamics within them, and as many definitions point out (Wolman & Leopold, 1957) the flat terrain neighboring rivers and streams that get flooded. As human developments increasingly occupy these areas, it is important for governmental authorities to create policies and plan their intervention, use and settlement.

Pinpointing the north most country of South America, Colombia is projected to be considerably affected by climate change (IPCC, 2007). Currently (Jan./2016) Colombia is experiencing one of the toughest droughts on recorded history, while in other parts of the world El Niño phenomenon causes floods further in South America and the United Kingdom. During the Niña event of 2010-2011, the country received unrecorded rainfall which led to flooding and landslides. Figures of 4 million people affected and losses around USD $7.8 million (Hoyos et al. 2013) were estimated. Since then, national and international organizations have worked more around floodplain management and have tried to spatialize floodable areas and flood extents (IGAC; TNC, 2014). Most efforts are done on the Magdalena River watershed as it is the most populated in the country.With recurrent flooding impacts voices have been raised demanding for more regional approach in municipal (local) land management plans, especially in risk areas. Municipalities are still overcoming the effects of the La Niña event of 2010-2011 and at the same time one of the government's priorities is to improve conditions in the river to increase navigability.

Communities along the river in the floodplain depend partly on the wetlands and have had historical and current problems with flooding. When protection works, infrastructure and facility development is being done along the Magdalena River floodplain, water and flooding dynamics are rarely taken into account while planning. Impacts of modifying the river and floodplain go a longer distance than the immediate surroundings, and this perspective is lacking for big and small interventions on the river and its banks.

Dredging and channelization is going to be done potentially changing flow and overflow conditions. Little study has been done as the river works are a national priority. Another fact that adds to flooding plains problematic is that with growing agro industry and cattle grazing ranches, "improvement" of wetland conditions to gain land is done. It is common that individuals (land owners) intervene neighbouring plots in the floodplain and attempt to gain over it. Also affecting surface water flows, local and regional governmental mitigation and protection works have cut connections to the wetlands, drying and draining them, creating problems with the fishing community. Conflicts among stakeholders are common when it comes to land or water, increasing tension and social problems in the aftermath of extreme events.

The national geographic institute IGAC & hydrological and meteorological institute IDEAM, had the responsibility to generate the flood inventory for the 2010-2011 event. This layer is used as a hazard map and as a base for planning and environmental licensing (CI, 2015). It was done by visual interpretation at different scales with different images. As it is based during one flooding moment it represents a single observation in time and not the complete representation of the extent that may become flooded during prolonged periods of (extreme) rainfall upstream. TNC constructed a multilayer approach to the Active

River Area ARA and other initiatives (TNC, 2014). This product has constrains as it is based on the SRTM topographic data and missing dynamic water behavior. In 2014, ALMA & TNC worked on the delimitation of the river floodplain and used the first official dataset; still this layer is just a processed version of IGAC & IDEAM. Recently TNC has been working in a long term water balance for large wetland systems on a monthly time steps. SAR VISION is mapping water bodies with radar imagery and IHE Delft Institute has being performing research on the area, but the results are at the moment unknown as it is ongoing.

As a (complex) containing unit the floodplain is useful to visualize and acknowledge spatially, because it has certain characteristics and problems that make it different from the surrounding landscape. Even though the surrounding land has effect on the lower floodable terrain, some of the floodplain processes do not exceed certain limits; it serves as a reference outer boundary in the food simulation assessment and for real life land management.

Historical context on river and floodplain management

Rivers and floodplains were the base for ancient civilizations to establish and thrive. In our recent history, communities have settled close to water bodies as well, where cities and towns have grown on flood prone areas. Today after hundreds of years attempting to manage rivers and control them with dikes and infrastructure (Nienhuis, 2008), currently in Europe the trend has been to give room to the river for its water. European rivers under such control are taken as reference of development. Constraining them has been a common denominator. For example, Dutch river system control was already achieved between 1500-1800 following complete regulation and canalization (Nienhuis 2008). In recent years there have been investments in some rivers to reestablish parts of its original floodplain providing space to recover natural dynamics and buffer high water levels. Germany and other countries in Eastern Europe have also reduced river constrain and increased their space. In Colombia, in current months a multi-million project started with the principal objective to guaranty navigability in the Magdalena River by dredging and canalization works. It has been an ambition to control it, but with that priority environmental and social aspects are ignored when planning and designing river and floodplain interventions. It is important to adapt successful solutions from other places to the local conditions and learn from the impacts of river management in natural systems and society.

Colombia's rivers have had some history of management with success and failures. The Zenu civilization between X BC and XII AC (UNESCO, 2015) thrived maximizing the productive potentials the floodplain offered at the lower Sinu and San Jorge rivers. They modified flooding areas with a sort of fish bone dikes, to flood on high water levels and contain water bodies when the river receded. They based their productivity and livelihood on a successful floodplain and water management.

In recent history, development and infrastructure projects in floodplains and wetland areas have had considerable environmental impacts. Looking at the deltaic region; Canal del Dique, Cienaga Grande de Santa Marta and Magdalena River outlet at Bocas de Ceniza are three cases where altering water flows have had great environmental and socio economic impact (Figure 1). Along the central region Mojana, river works also have not achieved the desired control and is common to see dikes and structures hundreds of meters away from the river courses, but successfully altering floodplain and wetland surface water flows.

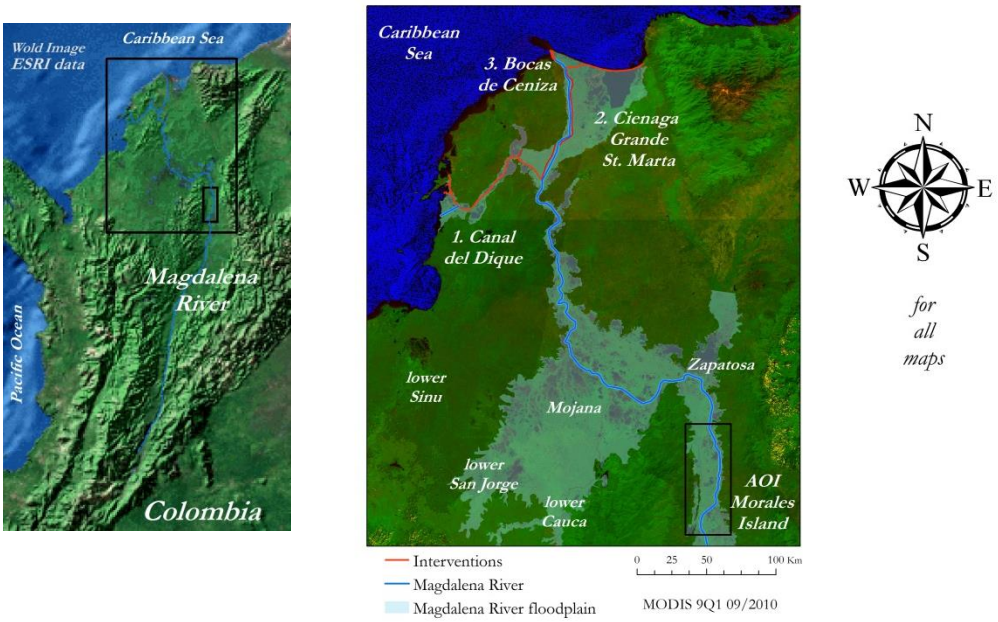

Figure 1. General location of interventions with high environmental impact in the delta floodplain.

During the Spanish colony there was a mayor modification on part of the deltaic area of the Magdalena River. Canal del Dique was constructed by attaching the wetland complex from the main river to the ocean to assure navigability through a channel. First works were done around 1650s, and posterior 1740s with Dutch design to connect the river with the canal avoiding a meander. Changing of that floodplain and connections to the wetlands and water bodies, has today great impact by the change in water flow, nutrient and sediment input. The original wetland configuration additionally filtered the river water and made it possible to have coral reefs at the outlet of the delta, which were covered by sediment. This area is considered of biological importance and has two national natural protected areas declared. Cartagena bay invests great amounts of money and national government has several projects to solve the problem. The redesign of the entrance of the canal built in 1740s is currently being done again with Dutch support by Royal Haskoning (2015/2016)

The Magdalena River creates a complex delta where Cienaga Grande de Santa Marta is an extense lagoon that limits with the Caribbean Sea with a beach coastline and mangrove forests. It was included a Ramsar wetland with international importance in 1998 (http://www.ramsar.org/es/sistema-delta-estuarino-del-r%C3%ADo-magdalena-ci%C3%A9naga-grande-de-santa-marta) and contains two other national natural parks. A main road was constructed (1956-1960) over the coastline connecting two capital cities that were separated by over one hundred kilometers of wetland. The road was made on a dike structure which prevented fresh and salt water fluxes that maintained the mangrove system. Additionally another road/dike was constructed along the right bank of the river to develop and reduce flooding on agricultural land. Development on the river side prevented water flow into the lagoon and with the years the system hyper salinized. Partial recovery was done in the 90s when flow paths were made along the road, other parts to the south remain saline and are hardly reparable.

The Magdalena River has its north most and biggest outlet at Bocas de Ceniza or ash mouths, name given by its murky waters flowing into the sea. Conditions in this branching delta made navigation difficult, risky and only possible on high waters. In the 1940s jetties were constructed to maintain the river outlet in one body. This created morphological changes in the coast to the west for over 100 km, where the erosion and accretion processes are still active today. The ecological impacts of those modifications are still unaccounted for. In the absence of channel connections, aquatic animals get their habitat reduced.

Common large animals in the lower Magdalena River are manatees, crocodiles, turtles and fishes that migrate up and downstream with the river pulse, in and out the lagoons through channels fulfilling their life cycle.

Not all wetlands and water bodies have to be connected through open channels, for example Cartagena city is beneficiary of a lagoon in the lower delta that has such a thick surrounding of mangrove forest that filters and provides fresh water that needs almost no treatment to be drinkable. For the maintenance of this ecosystem service this wetland provides, surface water connections have to be absent. All these situations at the end of the day have to be balanced for successful land and water management.

In September 2015 a conference meeting was held at Norte University (Foro Nacional Ambiental, 2015) to discuss about the environmental and socio economic impact of the river works that already started. In the press the constructing company promotes to have the final designs by the end of 2015. As the president declared this and other infrastructure works going on, as national priority, impact assessment is avoided and treaded too lightly.

1.2. Problem statement

For adequate management of the Magdalena River and its floodplain, is necessary to aim at an integrated spatial and temporal approach. At the base of such approach should be an advanced surface water and flood modelling tool. To aid such tool, the use of high resolution space born data can help to overcome aspects of data scarcity, as well as necessary field surveys and monitoring. Space borne data serves to represent system properties and aspects of geometry, at the same time to characterize land cover and to map flood inundation extents. Another appealing benefit of flood modelling is the simulation of events. Once the model is reliable it allows to simulate scenarios not only on (very) extreme climates, but also interventions on the river system. Many simulations around the river are for navigation related issues, while this research aims at urgently needed land planning and management applications.

By exploring different ways to represent the study area as accurately as possible, this work pretends to contribute in the understanding of the behaviour of surface water in the river and floodplain; by mapping and simulating water extents, together with making a specific link with discharge measurements. For adaptative management of a river floodplain it is useful to have a clear idea of the structure and functioning of the system; inflow and outflow points, what are the residence times, which are the water flow paths and wetland connections. Crucial also is to gain information on likely overtopping of dikes, breaching consequences and where to concentrate mantainance efforts, protection and modifications for water flow. Remote sensing, GIS and hydrological modelling provide suitable tools for surface water and flooding studies (Muniyanesa, 2014).

Adding to the research problem, the study area of the middle Magdalena River represents a case of low data accessibility, uncertainty on river measurements, and complex branching and interconnections between the water bodies. Lack of detail on the features that determine water flow, pose the biggest problems when attempting flood modelling under poor data conditions.

1.3. Research objectives

1.3.1. General:

Develop a 1D2D hydrologic flood model for the middle Magdalena River floodplain at Morales Island, with the use of SOBEK software (Deltares, 2014), remote sensing and GIS.

1.3.2. Specific:

I. Analyze the daily river stage and discharge time series to find and estimate return periods of specific flood discharges.
II. Test the usability of Landsat derived flood maps to evaluate the accuracy of simulated flood inundation maps.
III. Prepare a land cover map from Landsat, to represent surface friction as required by the flood model.
IV. Use the SRTM CGIAR DEM to prepare terrain elevation and to represent river banks for the flood model.
V. Set up and run the SOBEK 1D2D hydrodynamic flood model to simulate flood extents for selected inflows and selected model grid size.

1.4. Research questions

To reach the main and specific objectives of this research, some questions are formulated to guide it.

1.4.1. Return periods of extreme events

Which are the return periods of extreme events based on the analysis of the stage and discharge daily measurements in the study area?

a. *What are the return periods for observed flood events?*
b. *Are the time series of river stage measurements suitable to define return periods?*

1.4.2. Land cover, surface water and flood extent representation (optical RS)

Calibration and validation of flood models rely on available data on flood extent. To have information on spatial extent on areas that are flooded, maps can be obtained through remote sensing and GIS. With the application of satellite remote sensing, in literature it is often suggested that simulated flood extents can be validated by use of satellite based flood extent maps.

a. *For the selected dates, what are the flood extents mapped from remote sensing images?*
b. *Where and what additional information can be extracted from imagery to improve insight on identified flood events?*

1.4.3. Floodplain terrain representation (DEM)

Often the SRTM DEM is used to represent terrain elevation in flood model studies. DEM's, however contain errors, which some may need to be corrected to represent a floodplain's terrain.

a. *What is the difference between the IGAC Geodesy points and SRTM elevation data? Is it necessary to correct with the official geodetic elevations?*
b. *Can the DEM represent the floodplain correctly? Which are the mayor flaws? Does it need correction?*

1.4.4. Flood modelling

For accurate flood modelling many aspects of the real word that directly affect flood extents must be considered. In first instance, the river flow needs to be simulated. When the river has an acceptable behavior then the next step is to make interact with the terrain surface by overtopping and receiving flood waters. How water is entering and leaving the flood model domain, in the 1D channel or the 2D surface, have to be specified.

a. *Can the 1D river network correctly simulate measured stage and discharge? How can the 1D model be calibrated?*

b. *What is the effect of using homogenous or distributed surface roughness in the flood simulated extent?*
c. *What is the effect of upstream and downstream boundary conditions on the simulated river flows and floods?*
d. *What are the differences in flood model results when applying the 270 and 90 meter grid resolution?*

2. LITERATURE REVIEW

2.1. Extreme events and flooding

In large tropical catchments, natural water bodies commonly have significant variation in water level, according to the season and water inputs from the river, rain and ground water. Natural or "normal" variations on water bodies pose little or no threat to local communities, but the extreme low levels and very high levels can lead to considerable damage and loss. Meteorology, precipitation extremes and climatic changes combined with environment and anthropic factors will affect the water dynamics in floodplains and consequently populations associated to them, models can be applied to describe the processes that take place (Teegavarapu & UNESCO, 2012).

Maximum event analysis can be done depending on the objective and the behavior of the studied system or process. For example in the study area has a bimodal season, where extreme events happen in both of them. In an encyclopedia of Environmental Metrics (El-Shaarawi & Piegorsch, 2002) in the chapter of extreme value distribution, Pickles presents an example application with data (1911-96) from the River Meuse at Borgharen measuring station in the Netherlands. The first step was to prepare histogram plot for the daily maximum discharge to visualize the time series. Following, discharges lower that 500 m3/s were filtered out as they had no contribution in the extreme flow analysis. Afterwards another modification to the series was done attempting to get rid of the effect channel geometry change along the years. Measurement methods are also considered to have effect on the data through the time series. Vogel et al. (2011) go even further attempting discharge scenarios for the United States, modelling climate change and future modifications in the river and catchment. They consider how occurrence probability can change through time, considering also that records can have a different trend and do not contain recent extremes that have been experienced worldwide. Urbanization is made responsible for changing the river behavior and increased flooding. On the other hand Robinson et al. (1998) affirm that land cover changes have less effect on the hydrograph under extreme rainfall and floods, because the surface is near or saturated already.

Continuing with the extreme event method, in first place the daily values are processed and then the yearly maximum method is presented as a more common and a solution to avoid noise from similar values that are expected in a day series where there is dependence from one day to the other and other shorter ranges. The method of periodic maxima or block maxima is accounted as the oldest extreme value method analysis, they date it back to Gumbel, long history applications in hydrology. Gumbel distribution has been widely used for extreme event analysis. Flowing the periodic maxima, results in return periods of worst case scenarios, based on measured extremes. This indicator is easy to interpret, widely used and accepted. The identification of the blocks is important and generally is the same hydrologic year. On the example it starts in September and ends in August. This brings the question on how to set up analysis on bimodal systems, if it is worth to separate 2 seasons per year.

Recurrence interval or return period explains the probability of an event happening or being greater for certain period. If it is calculated for one year, the probable occurrence is the inverse of the return period.

For river and floods they are used to describe the how much water can be expected at a location and even relate to the magnitude and harm potential flooding has. Referencing to return periods is commonly done in legal and engineering contexts; for design and construction purposes. Scenario storm events or flood waves are elaborated in a specific range of return periods for different applications. Other indicator is the annual exceedance probability, is normally expressed in percentage, probability or as an annual recurrence probability which is the same return period (Garcia, 2015).

2.2. Landcover, surface water, wetland and flood mapping

Vegetation maps could be digitized or classified, depending on the final simulation area. Vegetation units can be digitized as it was done to correct for man-made features by Kanoua and Merkel (2015). Generating flood inventories is another important task to validate the simulation results. Interpreting, image classification and community based surveys can be useful to complete acceptable inventories. Vulnerability and exposure are also complementary parameters to include when overlaying the simulations with the communities that can be potentially affected by rising waters for risk studies.

In the context of flood hazard and disaster, water body mapping and monitoring has been approached from different perspectives with remote sensing (Joyce et al. 2009). Excluding visual interpretation, they can be summarized in two; optical (Huang et al., 2014) and radar (Hidayat et al., 2011; Melrose et al., 2012) based mapping. Methods range from the simplest to elaborate. Fraizer and Page (2000) successfully apply a method of simple threshold or density slicing on Landsat TM (mid-infrared band) to identify and delineate water bodies in southern Australia. This application is based on the different spectral response water has from other land covers. They argue that from the various methods of water mapping few studies do accuracy assessment with ground truth. They constructed their ground truth set with visual interpreted water bodies from aerial photographs taken on the same date as the satellite image.

Based on optical RS also in an Australian catchment, (Huang et al., 2014) uses MODIS as the principal data set together with Landsat imagery to map spatio-temporal flood inundation dynamics on floodplain and wetland ecosystems in the Murray-Darling basin. With MODIS they prepare the flood maps using the open water likelihood OWL (after Guerschman et al., 2011). The modified normalized difference water index mNDWI calculated on Landsat imagery as a contrasting set. They find that overall floods can be well represented but still MODIS is limited by the mixture of signals from surrounding materials and water depth. Relation of the water surface in relation with the size of the pixel is another source of error in their flood mapping. Aggregation is done from the flood maps on one event to produce a final a final flood map. Relating to measured high flows or peaks is also done in their study.

LIDAR data can also outline water bodies. Radar altimetry is another valuable complement for surface water monitoring (Da Silva et al., 2012), but not addressed in the research. Combination of elevation and land cover analysis for water mapping is also found in literature, for example in Ho et al. (2010).

2.3. Terrain elevation - SRTM DEM quality and aplications

SRTM was produced originally by NASA from a global survey with interferometric SAR C and X bands (Kolecka & Kozak, 2014), mounted on the space shuttle, hence Shuttle Radar Topographic Mission SRTM. The mission was flown between the 11th and 22nd of February of 2000 and took two years to post process (NASA). Since the initially released product had data voids on water bodies, steep slopes and topographical shadows, some filled products appeared. For example, the SRTM CGIAR (Consortium for Spatial Information) is advertised as an improved version of the original (http://srtm.csi.cgiar.org/). It has

void filling with new interpolation techniques and algorithms following Reuter et al. (2007). The spatial resolution of the elevation data is close to 90 meters per pixel.

Once global elevation data was available, following research has been done on local validation. There have been work comparing with cartographical data (Jarvis et al., 2004) and/or field measurements (Gorokhovich & Voustianiouk, 2006). Jarvis et al., perform their study in Colombia contrast the DEM's elevations with base maps of the national institute of geography IGAC, TOPO DEM and field data. They perform numerous testing on quality, accuracy and usability on different study cases; generally in the mountainous area, on a national scale, catchment and local scale. They finalize by using the topographic data in rainfall runoff modelling. In conclusion they consider the SRTM an advance on global elevation data and perform well for hydrological modelling. Compared to base data, it is better than topo sheets of 1:50 and 100.000; detailed base maps had more detail, due to the spatial resolution.

Other cases base their validation sets on LIDAR data, which is considered a more reliable ground truth on terrain elevation. Applying LIDAR, an assessment was done in central Siberia by Sun et al. (2003), where less error than the official SRTM specifications is reported, having even better match on low vegetation and flatter landscapes. Like other studies, they detect and correct vegetation induced errors in elevation.

For Australia, Gallant and Read (2009) also report offsets induced by woody vegetation in the SRTM DEM which were corrected. In summary the way to correct those offsets was to subtract the surface elevation to obtain the terrain elevation, based on vegetation maps and DEM values of surrounding clear cut areas.

With strong evidence that tall and dense vegetation is captured in the SRTM elevation data, some applications have been done to derive vegetation biomass (Kellndorfer et al., 2004). They state that optical sensors lack the ability to penetrate through layers of vegetation translating into a difficult estimate of vertical structural measures such as canopy height as canopy becomes denser. Then studying the relation of density with height would be useful in the attempt to improve on the removal of the vegetation effect contained in the SRTM DEM. Even though the SRTM data has some limitations, it has been a widely used base for elevation, even for hydrologic modelling.

2.4. Flood modelling

Water movement within the floodplain is ruled by terrain, as an example Poole et al. (2002) approached it by detailed photointerpretation and mapping of the geomorphic elements and vegetation for posterior hydrologic modelling. For improved simulations corrections have to be done to the Digital Elevation Model to remove vegetation or include bathymetry (Rudorff 2014) as lake and river bottom shapes. Besides the natural forms (Costabile & Macchione, 2015) and infrastructure, for flood hazard assessment and floodplain management is useful to have tool to locate and estimate the minimum dimensions of flood protection structures (Vorogushyn, 2010) and predict how they will behave in extreme situations leading to failure. The results are useful for evacuation plans, loss assessment and flooding recovery efforts (Mosquera-Machado & Ahmad, 2007). Barriers also have an effect in the flow simulations, as infrastructure controls the flow along the plain and when they fail or breech, flood disaster situations can occur (Huthoff, 2013).

Some events can happen unexpectedly, but flooding dynamics of large rivers can be anticipated by discharge or water level as basic input (monitored or simulated). Having such a tool to dynamically map flood indicators is useful for development projects and land management. Simulating or forecasting water

flow is a challenge not only for flood assessments (Nash & Sutcliffe, 1970), Merkuyeva et al. (2014) affirm that is the base for flood risk management in risk reduction and environmental protection. They state that for efficient real time flood management, flow forecasting is the base for flood monitoring, control and warning. That is why the combination of monitoring, modelling and forecasting are important, favored by the advances on technology, remote sensing and GIS software.

For the research, breaching and overtopping is considered the mayor causes for flooding and filling of water bodies. Flood happens differentially where intensity of the event, protection structures and exposed elements meet. To include the natural and artificial structures that control surface water flow (Costabile & Macchione, 2015; Poole et al. 2002; Poretti & De Amicis 2011; Syvitski et al. 2012; Rudorff 2014) is a task to accomplish for correct terrain representation and flood modelling.

For the Magdalena river in Colombia, Alfonso (2010) sets up a MIKE one dimensional 1D model to simulate the river together with the floodplain. Measured river cross sections were extended around 2 km using the SRTM DEM (90x90 meter/pixel) as floodplain terrain. It is a research done as one case in the study of model performance, validity and method implications for design and monitoring networks. The model schematization is done on the main river branch and lumped values for different river branches and wetlands are assigned. He defines the slope of the AOI of 33 cm/km and right after the lower boundary, slope decreases to 16 cm/km. Economic activities and conflicts are grouped as stakeholders relative to as navigation, fishery and agriculture, additionally flood control. A description and quantification of average fiver flows between connections of the main river, branches and wetlands is done. The monitoring system is also described. He comments on several points like measurement uncertainty, deficient geo-position and datum related stations, modification on the river and floodplain has considerable effects on the measured series recommending care in their analysis. Problems with outdated rating curves have been noticed and a common solution has been to remove old records to achieve a somewhat a constant hydraulic section where morphology has changed. A critic to the flood control works is done, explaining how the river constrain and blocking the floodplain reduces conveyance in the channel and increased river and flood stages. Reduction of storage capacity is another impact described. For the hydrodynamic model, rainfall is considered beyond the objectives of the research and not included. Wetlands were schematized in final simulations as storage units behind controlling structures to allow exchange along the high and low level seasons. Simulations were run with 10 minute time steps for one month, performing calibrations with the Manning value which go from 0.02 to 0.04. Concludes with the limitations of the model being basically attributed to unreferenced water levels, cross section consistency and floodplain description, changing river morphology vs. rating curves and complete assumption on wetlands.

Karim et al., (2011) perform hydrodynamic modelling on MIKE 21 to estimate floodplain inundation in one of the largest catchments in Australia. They saw how the Fitzroy river can swell up to 15 km across the floodplain. Although flooding in the catchment is not frequent in this tropical basin, one of the largest recorded floods was in 2011. The selection on of the study area was done based on the high ecological value the links of the river and associated floodplain have. Aquifer recharge is another consideration in this catchment. They base their elevation surface on a processed SRTM to 30x30 meter/pix, but resample again to 90 meter resolution for computational reasons. Vegetation offsets are removed and drainage enforcement is done, even on the floodplain. They had the advantage of performing LIDAR surveys on important places that determined water flow to increase the detail on the terrain and river geometry. Surface roughness coefficient was assigned to a land cover map which they constructed from different RS sources. For ground truth data, river stage measurements were used. They use the MODIS and AMSR-E imagery to validate the simulations. For the MODIS (day reflectance) imagery they write a code to remove clouds from images. They had to rely on interpretation and hand mapping when automated processing

failed to acceptably spatialize observable floods on noisy images. There is where the complementary coarse (10 km) passive RS aids water mapping. They describe their results as preliminary and that work would be done to better calibrate the model. The model results show overestimation of the river stage at some parts. After the flood extents were obtained, they were combined with the DEM. They affirm that their applied method helps address data deficiency vs. calibration and model requirements. Their final application with hydrodynamic modelling was to investigate hydrological connectivity of the Fitzroy river floodplain with its wetlands and ground water recharge to the aquifers. Well managed floodplains can help increase flood protection, aquifer recharge and improve habitats for wildlife (TNC). MIKE's main strength is stated as its capability to deal with changing soil moisture in the floodplain on flooding moments, as well as being able to handle even millions of computational points. And point its main drawback by having difficulties in the stream channel representation misrepresenting small overbanking events. This issue deals more with the drainage network schematization than the software's capacity to deal with them, highlighting the importance of correct inclusion and representation of the main, secondary and minor drainage networks. Another issue affecting increased overbank flow is that the model does not work in a coupled 1D2D fashion and suggest using MIKE flood to overcome it.

For the lower amazon river floodplain Rudorff et al., (2014) to integrate the river and floodplain behavior they set up a 1D2D LISFLOOD FP. This model is described as the simplest, and first application was done on the Dutch Meuse River between Borgharen and Maaseik (Bates & De Roo, 2000). For the case in the Amazon, the SRTM was used in combination with bathymetrical maps based on extense sonar surveys. They emphasize the importance of integrating elevations from terrain and underwater surfaces, and expose how challenging the context of data scarcity is and vegetation interferences are problematic in modelling inundations in floodplains. They find that by assuming channel geometries where there were gaps, the river stage was not affected considerably, at least a smaller error than the annual amplitude of the flood wave. They use Manning's roughness assigned to classified land cover types; open water, shrub, forest and two mix zones. They include at the final steps a water quality analysis where sediment and nutrient budgets are considered. The authors claim that it is the first case to simulate the flooding dynamics of the lower amazon successfully.

Studies have been done using different setups. For the Rhine River, Te Linde et al., (2010) apply just the 1D schematization on SOBEK for flood peaks to assess the effectiveness of mitigation measures along the river. They explored the probabilities of rare events and constructed scenarios. If flooding happened upstream, downstream the simulated flood peak will be decreased significantly as well as the discharges. They ran different waves obtained from statistical series build for thousands of years. Finally 4 scenario inflow boundaries at 4 locations with return periods of 10, 200, 500 and 1250 were run. These return periods obey to the legislation. They change attributes relating the meanders, by-passes, polder retention and land cover change on their simulations. They comment about humans already modifying the river since the Roman era and then making a more detailed timeline on recent interventions. Recently with flood reduction purposes downstream, upstream was canalized. For navigation purposes the river was straightened more. These changes in the river section & network caused higher speed on the advancing wave, putting the downstream at higher risk. They point out that land cover change to urban cover has and will increase water overland water speed. They put the example of one flood with and without protection works where at the location of Worms the peak discharge of the 1882/83 and 1955 floods differ considerably. The first is a wider peak of ten days reaching a peak close to 6000 m^3/s, contrasting the peak after dike rising where the peak is around three days faster and 2000 m3/s higher, it also recedes faster. In another research Oswalt & King (2005) evidence how floodplain and its forests in a Tennessee river in the USA have been altered by canalization works. Te Linde et al., set up the river channel in SOBEK based on cross sections each 500 meters, including the current state of the polders. Calibration

was done by adjusting bed friction coefficients. To simulate the effect of water leaving the channel when a flood was designed upstream, the schematization consisted of polders with regulated inlet and outlet sources to receive the overbanked water and eventually return it to the river. Besides that, they raise the bank elevations to assure that the wave is kept in the channel for the policy assessments they later perform.

In Atlántico department, Colombia for his MSc thesis, Amador (2013) sets up a 1D quasi2D SOBEK model for a wetland on the Magdalena River. As it done in shallow water bodies is referred as "Quasi", in other words partially 2D. He includes water bodies as high flood risk zone which might be useful to differentiate in hazard maps and defining flood risk zones. SRTM elevation data was complemented with bathymetry surveys and some dike measurements, but augmenting the area is full of interventions, only some were spatialized with correspondent elevation. Lacking elevation data on the interventions is considered of the main limitations on model performance, which still was considered satisfactory.

The combination of a model that can handle the river behavior together with the overland flow gives then the possibility of a more realistic model. An example of the application of 1D2D SOBEK model is done in the Lake Tana basin in northern Ethiopia, where data is scarse (Tarekegn et al., 2010). It is the largest water body in the country and source of the Blue Nile with a catchment of 1586 km^2. The Ribb River is the one with more water contribution to the lake. Flood simulations on the last 20 kilometers of the Ribb River were done. Flooding on the river plain is a repeating situation in the study area. Long flood duration and high impact is recognized for 2006. High water levels in the lake created a backwater effect that increased river bank overflow. This event was objective to simulate with hydrodynamic modelling, remote sensing products and GIS techniques to prepare the model inputs. Elevation data for river and floodplain terrain was based on the ASTER DEM (15x15 meter/pixel). Two basic objectives are set for their research; in first place the usability of the elevation data for two dimensional modelling. In second place for this complex area, the effectiveness of the constructed model for simulation of extreme flood events was studied. Together with historic flood extent location points, MODIS derived flood maps are used as ground truth, but conclude that the RS product used had too much uncertainty. Even thin water layers after rain events could be represented as flood extents, proving how sensitive remote sensing can be to water. Another identified difficulty is that simulations are data demanding and the output of any modelling is determined by data quality.

Another example of 1D2D SOBEK application is done in an MSc research project by Manyifika (2015). Contrasting from the previous application, this study area is a small and urbanized floodplain in Kigali, capital city of Rwanda. This model has issues with 1D channel calibration that translate into overbanking in places where in reality does not happen (Rientjes, 2015 personal communication).

Many of the studies consider geometry and roughness parameters to have the greatest effect on simulation results. Errors and uncertainties are contained in the schematization and boundary conditions, as well as measurements and observations.

3. STUDY AREA & DATA

Middle Magdalena, Colombia – South America.

The Magdalena river catchment is the most populated and is the largest in the country. It is large enough to be to be considered in global discharge and sediment budgets (Restrepo & Kjerfve, 2000). The Magdalena River flows River flows north into the Caribbean ocean where it ends in two deltas (

Figure 2). It has two mayor valleys; Cauca and Magdalena Rivers (Figure 1). They both join in the lower Magdalena complex of open and extense wetlands. With dimensions around 75 by 20 km (1900 km^2), the study area is a section of the middle Magdalena at its lower end. Middle Magdalena can be defined from where lagoons and flat floodplain appear, but still contained in a wide valley. Tributary catchments of the study area are estimated on to be 9944 km^2 and a contributing catchment of 127,490 km^2. To contrast with European catchments, the Rhine has around 185,000 km^2 (Te Linde et al., 2010) and Elbe 148,000 km^2, the complete Magdalena catchment has around 257,000 km^2 (Restrepo & Kjerfve, 2000).

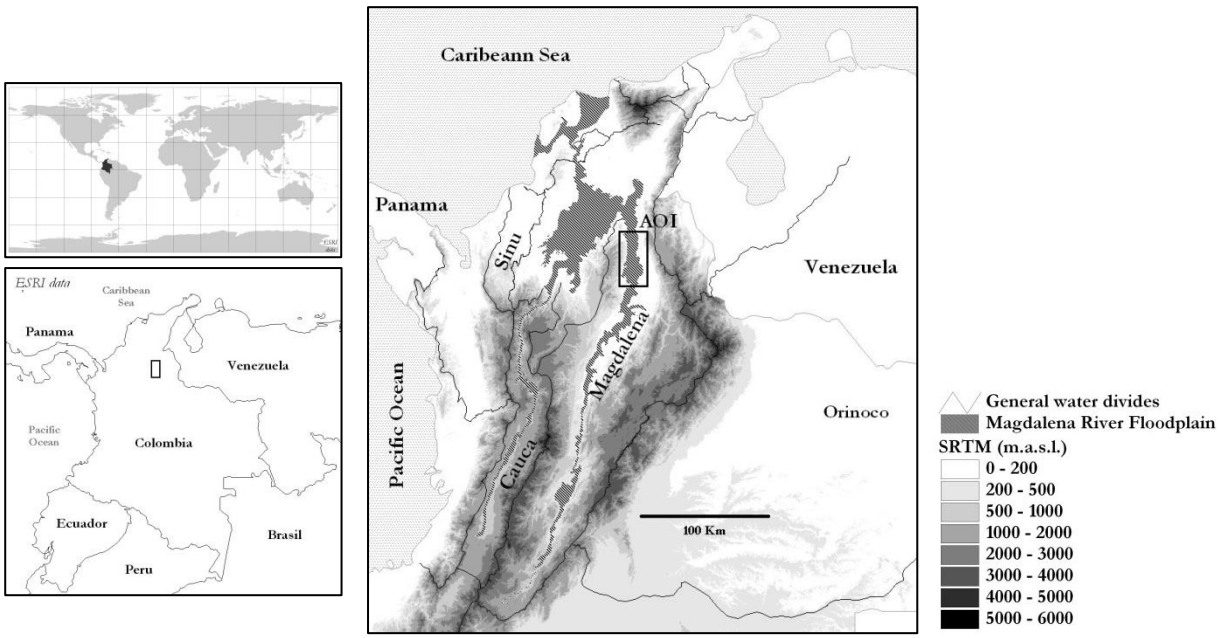

Figure 2. General location; Colombia, catchments, Magdalena River floodplain & study area AOI.

3.1. Study area

The selected area of interest AOI; Morales Island is in the middle part of the Magdalena catchment. It gets its name from Morales town and is called an island literally because of its river enclosure. The AOI has four (1-4) river gauges in a configuration that permits measurements in a single branch of the river (Figure 3), where the water goes in the defined floodplain and where it goes out, in between those two point the river diverts and connects to lagoons and back swamps.

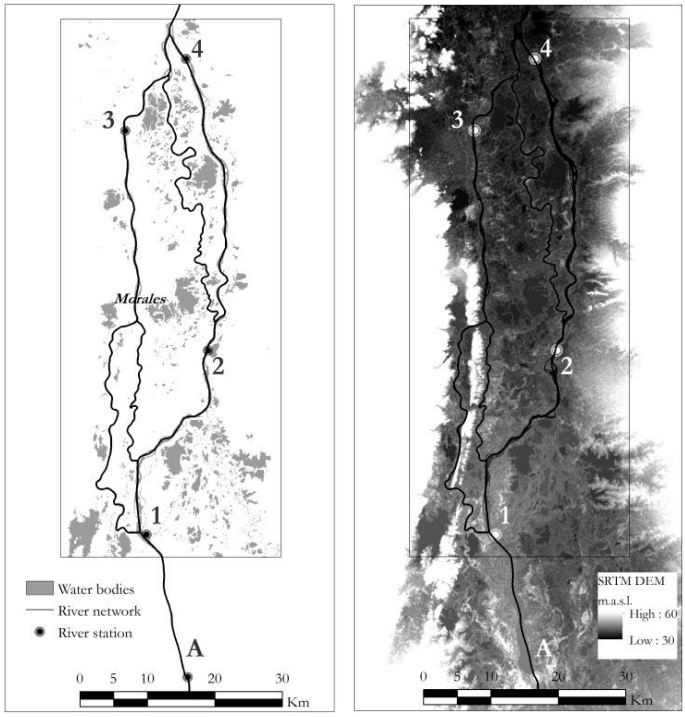

Figure 3. Water bodies based on Landsat January 2001 (left) and topography (SRTM CGIAR) of the study area (right), with the river gauges

For the study area, it is assumed that (1) there is no mayor leakage of surface water to groundwater, as for example Gieske (2009) assumed, as well as not accounting for rainfall and evapotranspiration terms focusing on the surface flows. Precipitation in this case will be accounted over the study area as additional input for the selected dates when data is available. (2) Surface water flow and flooding is determined by the water input of the main river through overtopping and breaching. (3) Lateral tributary drainage is not considered an important water input to determine large water overland flows in the floodplain.

The local climate is considered warm and arid, where pan measured potential evapotranspiration doubles the annual precipitation of 1000 mm (Figure 4). Potential evapotranspiration is higher in the beginning of the year with values of 200 mm, and decrease with the rainy seasons where relative humidity increases. Elevations range from 27 to 50 m.a.s.l. and the average temperature is around 29 ^{0}C. Station A shows general wetter conditions to the south of the AOI.

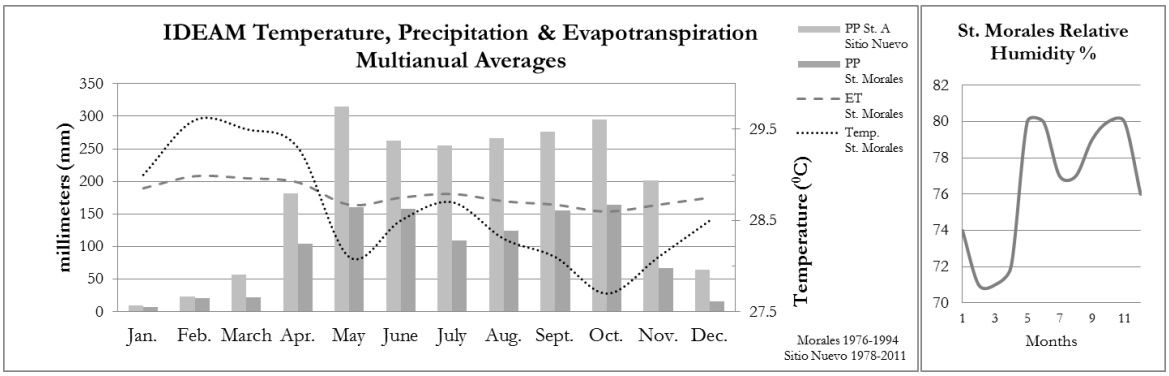

Figure 4. IDEAM data, monthly multiannual averages.

Hoyos et al. (2013) describe the lower Magdalena River valley with a high degree of flooding as well as high social vulnerability related with low values of living conditions (Goosen, 1961). There are 5 municipal capitals in the AOI and several other settlements. Throughout the rural area, there are disperse houses and agricultural activities which are exposed to floods. Rural and urban populations are permanently exposed to rising waters and their effect. Interventions are done on the floodplain and river, which can have changing consequences for the present water flow paths and wetlands. Fishermen, cattle ranchers and farmers and agro industrials are in permanent conflict because of their different water needs. (http://www.elheraldo.co/bolivar/secuestro-no-eso-solo-se-lo-hacen-los-ricos-240520). Taking an example testimony from a recently interviewed fisherman from Morales town; problems of lagoons drying up began after 2008, after the flood mitigation and protection works were done on the banks, blocking connections from the river to the streams that naturally feed the wetlands. These walls serve palm oil farmers and cattle grazers to transport their products, but have dried the wetlands.

3.2. Available data

The basic materials or raw data inputs are listed below. In the methodology section, for each thematic or processing block of the research, their use is described by steps. First the extreme event analysis with stage and discharge data (4.1), then (4.2) the Landsat derived maps for two main objectives; river and surface water extent and the other dealing with land cover to surface roughness. The third block (4.3) deals with the elevation data work and the last block dealing with the 1D2D flood modelling (4.4).

3.2.1. Stage & discharge data

The national institute for environmental and meteorological studies IDEAM is the one responsible to monitor water resources. After many discussions that arose since 2010/11, finally it opened some river gauge time series in the internet. Daily discharge and level measurements are available for 4 stations inside the study area. There are other stations that would be objective to obtain in the field work. The data is from 1975, 91 and 95 to 2012, they have some minor gaps that should be filled. IDEAM monthly data was also used to contextualize the general climate.

3.2.2. Remote sensing data

Landsat TM & ETM imagery: Landsat images with resolution of 30 meters per pixel are the base for land cover, the river network and map the water bodies and flood extents.

MODIS imagery: The obtained (AQUA) products with resolution of 250 meters per pixel are; 9GQ daily surface reflectance, 9Q1 8 day composite surface reflectance, and 13Q1 16 day composite NDVI. Some images were compared and selected on peak dates to observe its application in flood extent identification and normal water conditions. A high temporal resolution compensates their low spatial resolution.

Elevation data: SRTM DEM 90 meters is the base for the 2D modelling. Considering the size of the study area the resolution is appropriate (92.38x92.38 meter/pixel). Similar working resolution was seen on a field visit to the Rijkswaterstaad, which is part of the ministry of infrastructure and the environment in the Netherlands and is responsible of the design, construction, management and maintenance of the main road network, waterways and water system.

3.2.3. Institutional and other data

IGAC Geodetic points: The national geographical institute IGAC, has a database with points and elevations from geodesy surveys.

River sections: measurements from 2001 by CorMagdalena, the corporation that manages the complete river were facilitated by Dr. Leonardo Alfonso at IHE, Delft.

Social inputs and context: field visit to part of the study area in 2012, press and youtube videos relating flood events (especially 2011).

4. METHODODOLOGY

The method applied for this work revolves around preparing the required inputs to set up, run and evaluate the 1D2D SOBEK flood simulations. As it can be seen in the following figure (5), the work flow was organized in four basic thematic block; the river gauge record analysis, optical imagery to map flood evidences and land cover, digital elevation data and the core of the study, the 1D2D SOBEK flood simulations. The method within each block to obtain the inputs is described further.

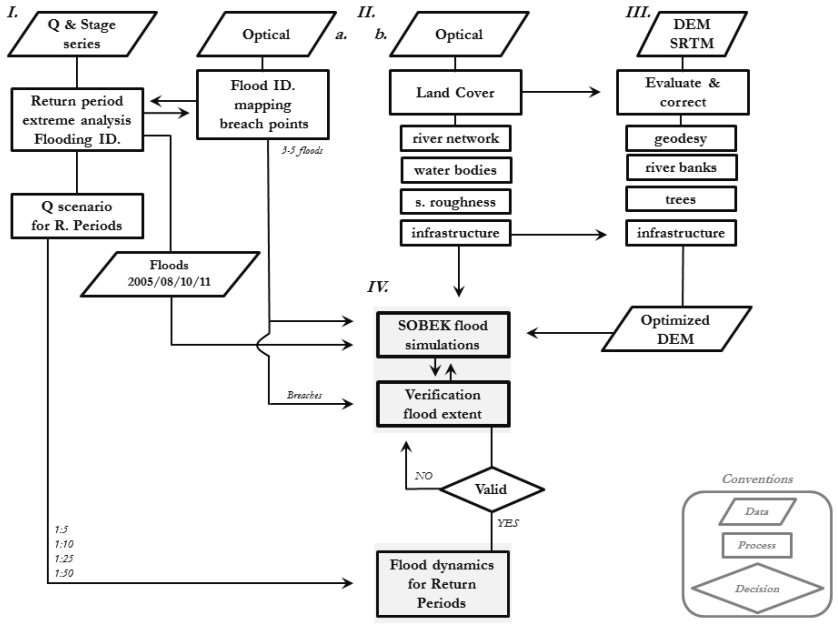

Figure 5. Methodological flow chart.

4.1. Stage and discharge data analysis

The Colombian institute of hydrology, meteorology and environmental studies IDEAM has the duty to monitor the water resources in the country. Recently gauge measurements have been open to the public. The stations in the study area and some in the surroundings were downloaded to study. Additionally from the KNMI Climate Explorer, rainfall time series were obtained from stations near the study area and were used in the initial phase of the research to observe rainfall activity on flooding moments, but work focused more on the river conditions.

4.1.1. Stage and discharge raw data

The general study area was defined for the branching system of Morales Island. Creating a bounding box and crossing with the IDEAM stations shapefile, the stations which were meteorological and not related to river measurements were discarded. From the complete river gauges, only four were inside the study area; two just with stage data and the other two including discharge. They were named Stations 1 through 4. Station 1, upstream and Station 4, downstream (Figure 6). These two stations only have stage or water level/river depth, daily measurements. The other stations 2 and 3 are in the main and second branch respectively and include daily discharge series. Branches are numbered with size and serve as reference.

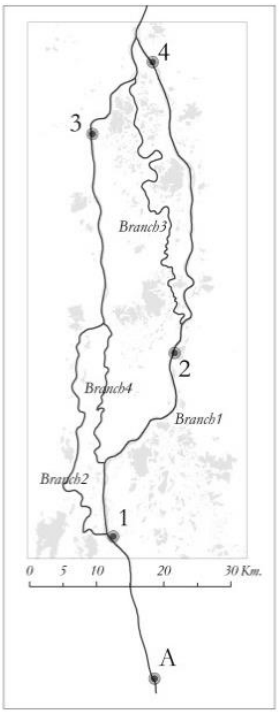

Figure 6. River network and location of measuring stations.

The other set of stations were downloaded after analyzing the first group, and were used to observe their pattern in relation to the first group of stations that showed similar hydrograph behavior. Two stations were on the river upstream and two other were on rivers that feed a wetland that later feed the main river branch south of Station 2 (Table 1). The only station that was selected from that group was Station A, and this station serves the purpose of inflow boundary conditions that can be seen later on.

Table 1. Raw data daily gauge records for the study area.

Assigned St. ID	IDEAM St. Name	Data type Stage / Discharge	Record Dates		Total Years
			From	to	
1	Badillo	Stage	1/9/1974	31/12/2012	38
2	El Contento	Stage & Discharge	4/2/1977	4/10/1977	36
3	La Nobleza	Stage & Discharge	1/1/1993	31/12/2014	20
4	La Gloria	Stage	1/4/1991	31/12/2015	22
A	Sitio Nuevo	Stage & Discharge	1/2/1979	31/12/2016	31

As the time series came in a matrix of days in rows and years in columns, the first step was to create a homogeneous vector that allowed correct placing of the daily records for each station, considering that there were also gaps in the records. Once the time series were organized and comparable between themselves, its quality was assessed.

4.1.2. Data quality assessment

As a first approach on the gauge series, general plots were made on different periods and on individual and grouped stations. The behavior of the hydrograph and stage measurements was observed, checking general consistency and congruence for different periods.

4.1.3. Extreme events analysis

Flooding situations always relate to extreme water presence in certain moment. In this sense the river conditions serve to contextualize and dimension known flood events and evidences captured with RS. To observe the complete distribution of the data, from low to high values, it was plotted daily. This option did not permit a good visualization of the data. Then a monthly maximum was obtained, but still was too many data. The last option which is found widely in literature was basing the Return Period analysis and Gumbel plots on daily maximum per year. Using the day maximum in the year, the Gumbel plots were prepared and the Return Period calculated for the yearly series. The top 10 ranks were selected from each station and analyzed.

4.1.4. Link imagery to flood discharge

From the pinpointed dates of the extreme event analysis, some high flood discharges coincided with recent and significant flood occurrences. Once having dates on significant flood events, remote sensing imagery was consulted on and around them to detect flood evidences. From the yearly extreme value, the daily series was analyzed on the hydrograph pattern to detect secondary peaks and sustained high waters to search also on those dates. Images that could show recession or two moments of flood increment, were also targeted.

As the main source for imagery, the Landsat database served an excellent purpose. From its resolution, date availability, access and sensitivity to water. As support and verification for what was detected in Landsat, MODIS products and images were also consulted, although spatial resolution is larger than for Landsat. However, by lack of field data on flood extends, MODIS images offer a fair option for the confirmation of Landsat based flood extent maps, obtained with higher resolution. With a high temporal resolution, MODIS in the other hand potentially permits to follow big flood events, with cloud cover as remaining inconvenient.

4.1.5. Water diversion across branches

After the extreme event analysis was done, further analysis was done on the gauge series. One important consideration is how much water goes through the branching system. Considering that there is only one inflow point, addition of the water in branches 1 and 2 should be equal to the flow before the branches divide. In this sense discharge from stations 2 and 3 were related to station A. This was done in part to detect the amount of water that was coming in the system and not measured as inflow at station A.

As an initial inflow point, Station 1 was set but had the problem of lacking discharge estimations. The correlation between stages at the two stations was tested with good results. Correlation values increased while restricting the time span; the complete data set had 0.88, using 2008-12 value increased to 0.96. And taking only the years 2008, 2010 and 2011 corresponding correlation values were 0.97, 0.99 for the last two years. Despite the good correlation, several methods were tested to obtain discharge at station 1, but the results were not consistent, there was too much difference from the extrapolated discharge at Station 1 from that of Station A, just 20 km downstream on a straight channel. After several tests it was decided to include the stretch up to Station A including it as the inflow point.

Stage and discharge relations analysis was done on Stations A, 2 and 3. Initially the stage discharge relation served as base to extrapolate the discharge at Station A to Station 1. For the other stations, it served as an objective to calibrate the river cross sections in the 1D simulations.

4.1.6. Observed high flows at Station A

The high flow time series related to flood events for 2008 and 2010 are incomplete. The next interesting high flow event to simulate was 2005, but also has an apparent error at the start of the recession where it jumps and then descents linearly. The high flow for April 2011 was complete and was consistent in all the stations so was chosen as inflow for the simulations.

4.2. Optical RS for water and land cover mapping

ERDAS IMAGINE, ILWIS and Arc GIS are GIS & RS software used in the research to process satellite images, spatial data analysis and map preparation. The required river network, surface water and flood maps, were produced from the application of satellite RS and GIS procedures. Surface roughness for overland flow is another model input for inundation simulations. It was parameterized from a general land cover representation based on Landsat imagery.

4.2.1. River, water and flood maps (30x30 meter/pixel)

Visual interpretation is commonly applied to for mapping. In literature there are numerous examples where interpretation is used as a main way to produce maps and as a solution (e.g. Karim et al., 2011) where automated processing fails due to noise from atmospheric conditions, when the land or water surface is still visible below hazy or cloudy scenes. The same applications were done in this research.

After delineating the study area, the next step using Landsat imagery is to obtain the dimensions of the river and to digitize its branches. Together with the elevation of the banks obtained from the DEM (4.2.2.), this information gives the base to set up the branching channel system in the model. Breaching and overtopping locations were searched for and located, mostly breaching was visible and present in flooding and non-flooding moments. Towns and main road/dikes were digitized to have the possibility to overlay with results and use in final layouts.

To evaluate or validate the results of the 2D simulations, flood maps were produced for the selected high water flow dates identified with the extreme event analysis (4.1.4.). For the event of 2011, 3 Landsat images are useful and an interpretation was produced for the scene of May 09 2011. It was also classified but the cloudy conditions did not permit an acceptable result in the north western part. This scene captures the peak after a few days of recession. The scenes of April 23 and June 10 also show significant flooding.

Based on the clear spectral difference open water surface has with land, it was sufficient to perform unsupervised classifications on the images and later recode into water - no water maps. Besides the flood maps another set of water maps were produced to have an estimate of the extension of the water bodies when they are in a "normal" condition. To accomplish this task, final sets were constructed. One consisted in applying a threshold to merged water maps which were done in a previous personal work (ALMA 2015). Another was to select a scene that resembled the normal condition of the water bodies to classify. The first exercise was done with six images (**Error! Reference source not found.**). After classifying and recoding to water no water layers, they were put together and applied a threshold to remove where water was just sometimes present. This layer does not cover the complete study area, missing a part in the south. The other task on the image of January 2001, was to derive a water – no water layer with the same method. After obtaining the two layers they are compared to observe where they match and differ. The resulting water bodies were visually contrasted with official cartography on the IGAC website to have another source of "normal" extent.

Table 2. Selected Landsat scenes to derive data

Landsat scenes for water bodies	
TM	9-Mar-86
ETM	27-Jun-00
ETM	29-Jan-01
ETM	22-Feb-01
TM	14-Mar-11
OLI	1-Jan-14
OLI	4-Jan-15

Landsat scenes for flooding	
ETM	2-Dec-05
ETM	18-Dec-05
ETM	12-Jun-06
ETM	10-Dec-08
ETM	26-Dec-08
TM	14-Mar-11
ETM	9-May-11

Landsat scenes for cross sections	
ETM	3-Jan-00
ETM	4-Feb-00
ETM	20-Feb-00
OLI	1-Sep-15

Another application of these water maps was to assess the changing river and cross sections. Classifications from 2000, 2001 and 2011 revealed how the river had changed and most important at the gauge station surroundings and the connection areas. An example of a sedimented section was applied to the stretch of the river from Station A to 1, to run 1D simulation to test the observed change in dimensions of the river channel from 2000 to 2011. As a last product of Landsat classification "normal" water bodies were spatialized. An exercise using several images from different dates permits to identify where the water bodies repeat and persist in time. To observe with of these water bodies has currently dried up, the same analysis was done with a scene of September 2015 and January 2016, where most of the remaining water bodies have connections to the river. Water table plays another important role in the maintenance of water bodies; it defines the condition for surface water to act upon, becoming more important when surface water lowers to the point there are no channel connections.

To perform a check on the date selection and flood signal of the Landsat imagery, MODIS imagery was obtained. It was first assesses if the selected products reflectance daily and weekly products (9Q1 & 9GQ) could capture the water bodies of the study area in a normal condition (e.g. January 2011). Then the same dates of the Landsat data were obtained for 2011 and 2008, as well as the dates with highest peak for those years. This serves as a flood extent validation and complement, as well as a validation on the date selection based on the extreme event return period on the discharge data. The NDVI product (13Q1) was also consulted, as it low and null NDVI values are assigned to water surfaces.

From Landsat, the used bands were number 3, 4, 5 and 7 (Table 3). MODIS bands cover similar parts of the spectrum so they are spectrally comparable, having better sensitivity to water bodies on its second band. Landsat as well, has better capacity to detect water above the visible ranges, where water absorbs these wavelengths contrasting with vegetated and bare land that have high reflectance.

Table 3. Landsat and MODIS used bands (Landsat & MODIS specifications).

Landsat bands	wavelength (micro m)	MODIS 9Q1 bands	wavelength (micro m)
3 - Red	0.631-0.692	1	0.620-0.670
4 - NIR	0.772-0.898	2	0.841-0.876
5 - SWIR 1	1.547-1.749		
7 - SWIR 2	2.064-2.345		

4.2.2. Land cover / vegetation map (30x30 meter/pixel)

A general land cover map was produced for the scene of January 29 2001. The scene had no clouds in the study area and gave an accepted representation for the river network and vegetation. An unsupervised classification was run and later a reclassification or recoding into the general land cover classes was done. The final objective for the land cover map was to be translated into Manning's N friction coefficients, which was done based on literature. This last step required again the recoding operation within the GIS.

4.3. Digital elevation model DEM

The terrain elevation data comes from the SRTM CGIAR DEM product. The data was obtained and finalized by cropping the AOI. The dimension of the calculation grid for the flood simulations is of 33 x 80 km.

4.3.1. Quality and validity assessment

The main quantitative assessment on the elevation data was to contrast with the geodetic points available in the geographical institute IGAC website. This survey is made in pair points taken along roads and small villages where clear land cover is commonly present and relatively flat terrain. The AOI for this case was increased to the east side of the river; where there is more developed and are more control points. The points were selected, transcribed and produced a point shapefile to compared with the pixel values of the DEM. A scatter plot was made and the differences in elevation per point calculated, this last result was included in the shapefile as attribute. Each point was observed over the Landsat imagery and on Google Earth to observe the general land form and cover where they were measured, including the observations in the attribute table.

4.3.2. Application: Base for cross sections (1D)

Once the validity of the elevation data is accepted, it was used as the base for the cross section bank elevation. Points along the river with an even distribution were defined (Figure 7); additionally the points where the river diverts were needed to give elevations. A final distribution and definition was done in detail when point by point, elevation data was obtained from clear patches and assigned as bank elevation. Clear patches came from the visualization of Landsat images of January, February and March of 2000 and January 2001. In total, 24 cross section points were defined.

While retrieving the river bank elevation values from the observed clear flat patches, still higher than expected elevation variability was captured in the DEM on homogeneous plots. Measurement of that variability was done by digitizing clear and flat plots and analyzing the variance in elevations (ANNEX 1).

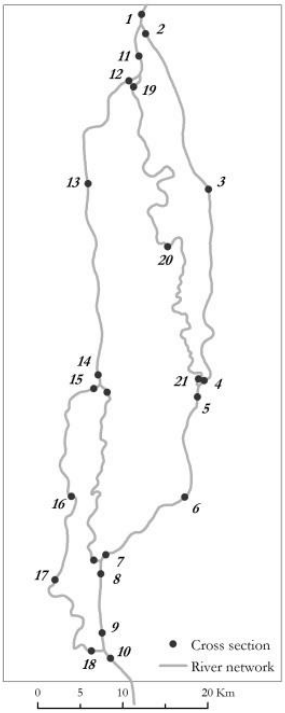

Figure 7. Cross section locations for the AOI.

4.3.3. River cross sections

Measured cross sections were available from CorMagdalena, but due to some issues described in the results, were not used and decided to design synthetic or model cross sections.

The geometry for the cross sections was obtained through two ways; the first was through an estimation of 6 meters deep river channel. This depth is based on press data which related other stations, literature on the river and other stations, and stage measurements (Annex 1). The second method gave convergent results with the initial design. Using Station 2, an estimate was done where for each meter in stage increase the increase in cross sectional flow area provided the model. This was estimated with an average velocity of 1 m/s. The same proportion of the design cross section was applied to the different points and river widths observed with RS, producing the dimensions of 24 selected locations. Several sets of cross sections were tested in the calibration of the 1D channel.

As a final step for 1D2D simulations, the slope of the main 1D channel was smoothened (Figure 8) as testing indicated that the model is very sensitive to bed slope gradients along the river system. Tests also served to assess effects of the downstream boundary conditions to allow drainage of channel and overbanked water out of the model domain. The same was done for the second branch.

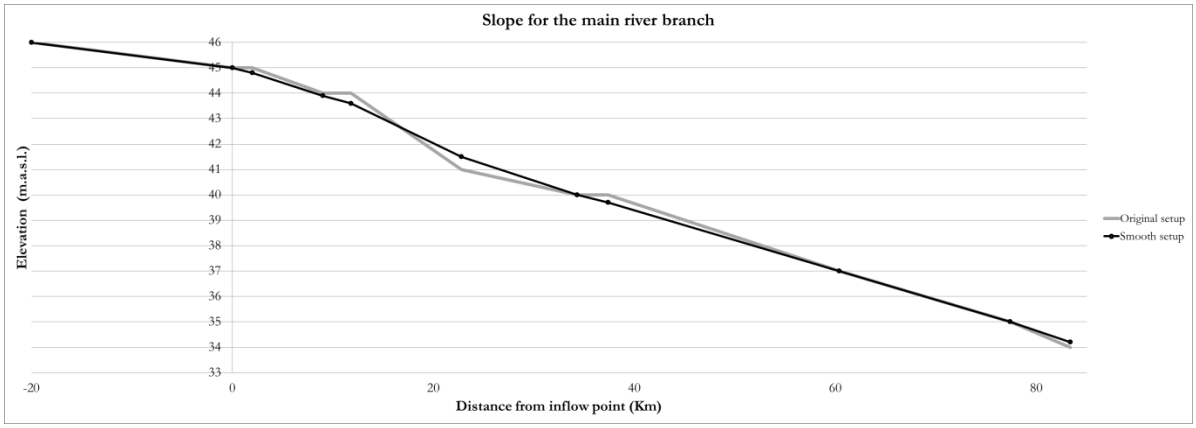

Figure 8. Initial and smoothened slope, main branch.

4.3.4. Upstream and downstream boundary conditions

Boundary conditions strongly determine model simulations as they define how the water is entering and leaving the model domain. They can be defined fluxes or heads, and have such strong effect due to the fact that they govern the overall mass balance of hydrodynamic flow models. For the developed set up, and in agreement with the SOBEK manual, the upstream boundary is defined as an inflow or Neumann condition with a time series of observed river discharges, to force the water mass into the model. The downstream boundary is defined by a Dirichlet condition or free flow with a fixed hydraulic head that allows water to leave the domain following downstream hydraulic gradient.

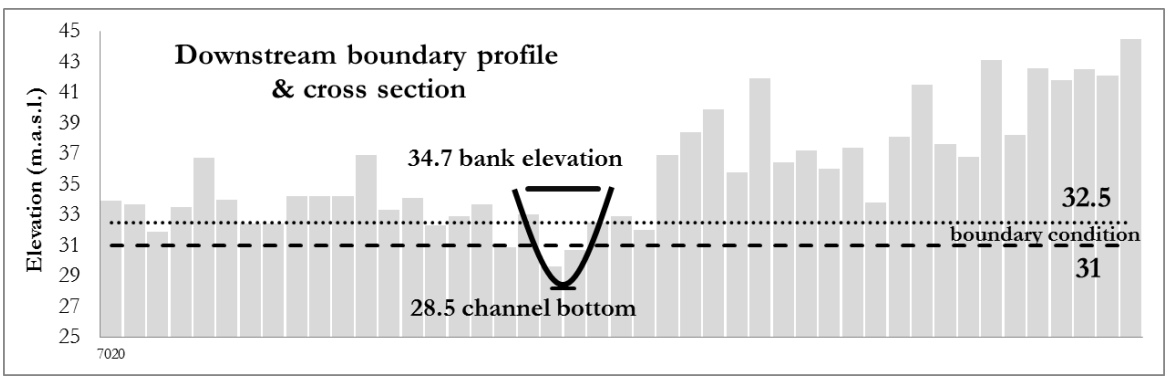

Figure 9. Downstream boundary profile (270 m grid), cross section and boundary conditions.

In the previous Figure (Figure 9), the boundary elevation data from the resampled 270 meter resolution DEM is plotted with the boundary conditions defined for the 2D runs. The last cross section is also plotted to observe their relation, although the cross section elevations just at the boundary are slightly lower considering that the cross section is located 4 km upstream. The initial conditions were set with 3 meters of water in the channel, which was an approximation using the observed series. The discharge on the first time step was also taken into account to be coherent with the initial stage.

4.3.5. Applications: Elevation surface (2D) input

From the initial 2D test runs, a problem with the river depth contained in the DEM was identified. The assigned elevation value of the water surface represented a unexpected water depth value as a result of a very low DEM pixel value; the elevation of the river was close and sometimes lower than the 1D river bed. A warning was issued by the software and the simulation reports suggested adjustment on the elevations for those pixels. A GIS pit-filling procedure was done to achieve an adjustment. From the cross section locations the river bank elevations were linearly interpolated and replaced along the main and second river branch, obtaining the DEM with the river bank elevation representation. The final step was to resample the elevation grid to 270x270 meter/pixel for the first set of flood simulations. Cubic convolution, bilinear, and nearest neighbor interpolations were tested. Cubic convolution was selected after observing the differences that the differences with the original were less than when applying the other methods.

Vegetation offsets are another source of error to consider as in many literature is evidenced, in the study are and its surroundings, it was also observed. Offset evidences are were observed by comparing the elevation of neighboring patches of tree and grass or bare covers. Digitized units of homogeneous land cover were crossed with the DEM to observe how variable the elevations were per cover class. Grass, tree, bare and sandy islands were analyzed. An additional unit where a thick tree patch was visible in 2000 but cleared on later years and observed flooded was also included to quantify its cover elevation.

4.3.6. Topography as indicator of flood prone areas

As a general indicator of flood prone zones, sliced topographical maps were prepared. These layers also help to have a general area to compare results in the discussion and also to mask non floodable terrain, getting rid of noise for visualizing and quantifying results. Three slice maps were prepared to separate elevations below 35, 45 and 50 m.a.s.l.

4.4. 1D2D flood modelling

SOBEK Advanced Version 2.12.002a, developed by Deltares is licensed software available in the ITC was used for the river and flood modelling. It is an integrated software package for river, rural and urban management (Deltares, 2014). It can handle any type of cross sections and combinations, being advertised that size and network complexity does not matter. The hydrodynamic 1D2D model bases on mass conservation and was made to handle any type of flows. Has the capability to model big rivers and flood events from breaching and overbanking.

The SOBEK model is constructed under a set of equations that permit 1D2D water routing along a channel and if the water in the channel overbanks, flow over the terrain is calculated. In the core of all computerized flow routing simulations, the Navier-Stokes equations are used (Gilles & Moore, 2010), which are used to describe movement of fluids, applying Newton's second law. The 1D module works on the complete Saint-Venant Equations, which are based on momentum and mass conservation. 1D can

handle backwater situations. For the 2D calculations surface roughness is applied. For further documentation Deltares web page provides the links.

In the SOBEK software, flood depths are already simulation outputs, while Karim using MIKE after the flood simulations, they overlaid the flood extent with the DEM to obtain flood depths.

The SOBEK model was set up based on the tutorials available on the help files and an online draft (Deltares, 2014). After being familiar with the basic buttons, the first task was to set up the river network 1D schematization. Once finished running and as well getting familiar and calibrating the model. The 2D scheme was worked on. Their integration took some time and after solving set up details, the model was ready for the final simulations. Before this last step, final adjustments were done to the model. The final simulation conditions and tests were defined and simulations on the initial test resolution of 270x270 meter/pixel were done, finalizing with the 90x90 meter/pixel resolution. Along the model development, parameter changing and testing 1D & 2D results, was the core of the research.

4.4.1. 1D schematization

The 1D river network construction consists of two basic inputs; the river network and the model design cross sections (24). Within the SOBEK software there are several ways to set up a river network and assign boundaries for a study area.

AOI definition / boundary locations; inflow (Q) and outflow (stage)

In the study area selection, the configuration of the river and its boundaries was taken in mind. The AOI meets the criteria of a floodplain that has a complex flooding behaviour with clear and simpler inflow and outflow points, which were measured. One inflow boundary node that is determined by discharge fluxes and another node for the outflow boundary (Figure 10), set to force a fixed head. For the 2D setup an additional line boundary was expanded along the downstream boundary of the study area to allow overland flow to drain with a fixed head.

Connection nodes and branches

Branches are the basic units for the river representation. Branches connect and complete the river channel or river network. Connection nodes permit two or more branches to be fused. For this case the setup consisted of 4 connection nodes and 9 river stretches.

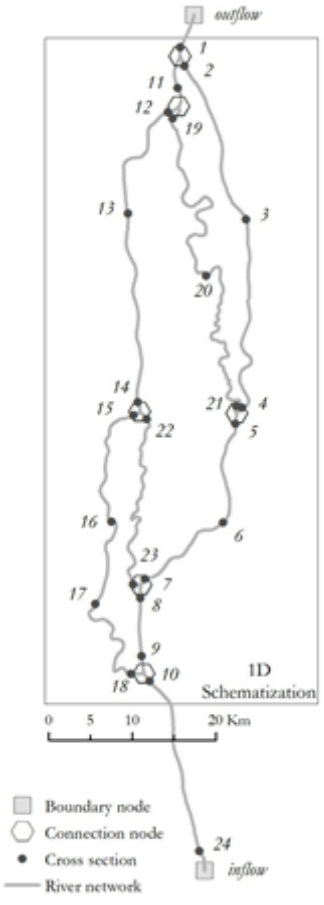

Figure 10. River network schematization

Cross section location selection and data to describe river bed and banks (geometry/profile)

Measurements of cross sections were evaluated contrasting with the general elevations from the DEM and with the river stage record range. As the measurements had too much uncertainty and mismatch, it was decided to proceed with model cross sections to describe the river bed and banks for the 1D schematization.

A U shape form had to be designed with a maximum depth of 6 meters. This average depth is concluded after having in mind different river stages that appear in press, the IDEAM webpage and measurements. The first design was done on a stretch of 300 meters (Figure 11) and the same proportion applied to the observed river widths at the 24 specified cross section locations (Figure 10).

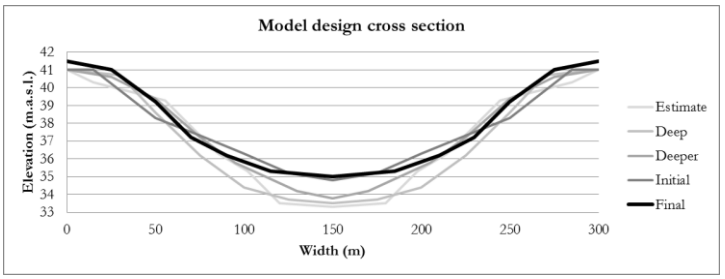

Figure 11. Model design cross sections.

Stage discharge relations

The only ground truth about the cross sections was contained in the river stage discharge measurements. From simulations with the initial cross section and continuous inflows on steady state mode, stage discharge plots were made for the station location and other check points along the river. Attempting calibration, this was repeated with changing the cross sections geometry to fit the observed stage discharge curves for stations 2 & 3. After several tests and results were needed to proceed, a final dimension was selected to run the 2D simulations.

In aims to obtain a more realistic representation one more fix was done to the selected cross section set. The general slope was checked and smoothened. Elevations of the cross sections on connecting nodes were equal, thus making those node neighborhoods completely flat. This was an objective while making the model set up, but for the final model the general DEM slope was included.

After making the final adjustments, changes in boundary conditions were tested. Extreme high and low inflows were combined with extreme high and low head at the outlet. The effect of the backwater effect of having a high head at the outlet was observed and can generally affect around 30% of the river reach. The elevation for the downstream boundary was selected on 31 m.a.s.l.

River cross sections and partitions

From the measurements of stations 2 & 3, a percent or partition relation can be established. This flow percentage on each river branch was additionally used as calibration criteria for the cross sections that connect branches (Figure 12). Water distribution on connection nodes is done according to the cross sections geometry and interpolation and no other forcing was made. An acceptable partition of the river flow is of around 70-75% in station 2 and 25-30% in station 3.

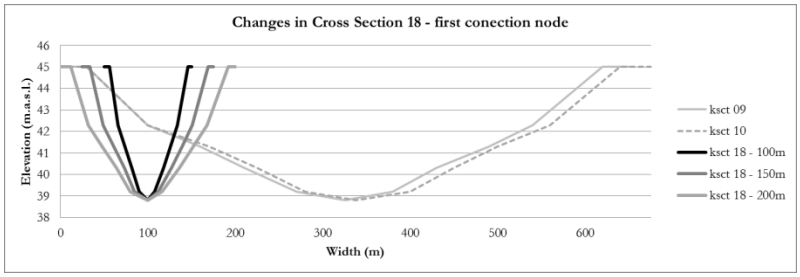

Figure 12. Changes in cross sections on connection point, example cross section 18.

River cross section's surface roughness - friction; Manning's N

Another calibration criterion was timing. According to the measurements, the peaks present in upstream stations are detected the next day at the stations downstream. Changes in Manning's friction coefficient were done for the river network, and observed that acceptable values were between 0.02 and 0.03. The latter being too high, 0.025 was selected. For the final 1D2D simulations, 0.02 was selected, having in mind that with higher values, river stage was overtopping too soon. A sacrifice of timing for a more realistic river stage was done then.

The surface roughness or friction values compared with the reviewed online tables after Chow 1959 and pictures of the USGS paper 2339 (Arcement, Jr., Schneider, & USGS, 1989) For reference one PhD (Alfonso Segura, 2010) research and another MSs (Manyifika, 2015). A higher value was expected to be used for the channels, due to the fact that the river schematization does not contain islands and is a smooth homogeneous U shape along all its sections. Higher and lower limits were tested.

4.4.2. 2D schematization

After preliminary testing and river bank elevation inclusion in the elevation data, the final 2D schematization was done. Two working (grid) resolutions were used; 270x270 meter/pixel resampled from the original 90x90 meter/pixel. Initially the surface roughness is left homogeneous and later parameterized by means of general land cover units. Test on multiple resolutions is recommended and can be done with more time and computing capacity for a more complete sensitivity analysis.

Preliminary test on smaller areas with 90x90 meter/pixel resolution

Before running the day timestep and complete study area, trials on smaller pieces of the AOI were induced overland flow to observe general overland flow pattern in smaller timesteps. The effect of slight higher elevations of tall vegetation pixels was detected, by surface flow going around and limiting those pixels.

Run tests on steady state upstream boundary condition

The first runs on the complete study area consisted of evaluating the flood extent which resulted from steady state inflow as the upstream boundary condition. For presentation three runs were done incrementing the discharge for each case (3000, 3500 and 4500 m^3/s) and the embankment option turned off in the 2D module setup.

Run test on measured inflow (with and without embankments option) upstream boundary condition

When the model proved it could run, the river discharge from station A was defined as boundary condition for the first five months of 2011. The simulations were done without and with the embankments option to observe the difference in the resulting flood extent.

Run test on observed inflow as upstream boundary condition (with embankments and distributed friction)
To continue with the grid schematization, distributed friction values were parameterized according to the classified land cover units and values found in literature. The flood extent was then compared with the result of using homogeneous friction values with the same upstream boundary conditions.

Evaluation / Validation
For final presentation and quantification purposes 1D2D simulations are run on the coarse and detail prepared grid resolutions. To evaluate the 1D run with the final cross section and parameter set, the complete year of 2010 was simulated and contrasted with the observed series at Stations 2 & 3. To establish the difference of the 1D results when functioning alone and coupled to the 2D module, results from the simulation of January to May 2011 were analysed. For the 2D flood simulations the final period was from the 1st of March to the 31st of May, attempting to reduce calculation time preparing comparable results. The resulting simulated extents are compared on a pixel level, between simulated with different settings and observed flood extents. Six tests were performed as a sensitivity analysis on the friction parameter, boundary conditions, resolution and finally two cases contrasting simulated and observed flood events for 2005 and 2011. 2005 was simulated on the 270 meter pixel and 2011 was the only case where the 2D simulation was done with the 90 meter pixel scheme.

1. Change from homogeneous to distributed surface roughness
2. Changes in upstream boundary condition
3. Changes in downstream boundary condition
4. Changes in resolution
5. 2005 flood event
6. 2011 flood event

5. RESULTS & DISCUSSION

5.1. Stage discharge time series – extreme events

From the analysis of river time series important information was extracted to continue the 1D2D model set up. Calculation on the return period of high flows were obtained for the stations, stage discharge relations were established for the calibration of channel geometry, it also gave the insight on the river flow diversion along branches and finally indicated the dates for further search on the satellite imagery for flood evidences.

5.1.1. Stage and Discharge time series

As most of the water that flows through the study area passes through Station A, measurements at this point are a good indicator of the hydrologic conditions of the study area and the Magdalena catchment upstream. The raw discharge data matrix can be visualized and seen in Figure 13Figure 13. The dry period of 2010 and posterior high water level moments are observable in the darker groups at the end of the series. In the first fourth of the bar, there is also a darker aggrupation, showing more continuous months with high discharges. On the other hand whiter sections along the bar indicate drier conditions in the catchment and lower discharges.

Another way to visualize the complete discharge records of station A, was to prepared histograms with classified and complete data series. The mean of the measured discharge is of 3654 m^3/s. 50% of the measurements fall in the range between 2000 and 4000 m^3/s. By grouping in classes the real data gets filtered, but then is just matter of defining the thresholds. Classes in this case were defined with arbitrary increments of 500 m^3/s. Another range classification can be defined with densities. For example two distinct groups can be seen around 2500 and 3200 m^3/s on the detailed histogram (Figure 14), and can be worth separating depending on the objective. The extreme peak discharges (5.1.2.) are only present in around 2% of the records.

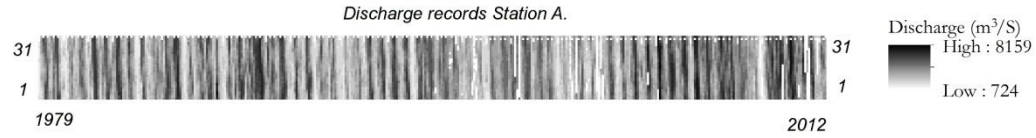

Figure 13. Station A discharge raw data matrix.

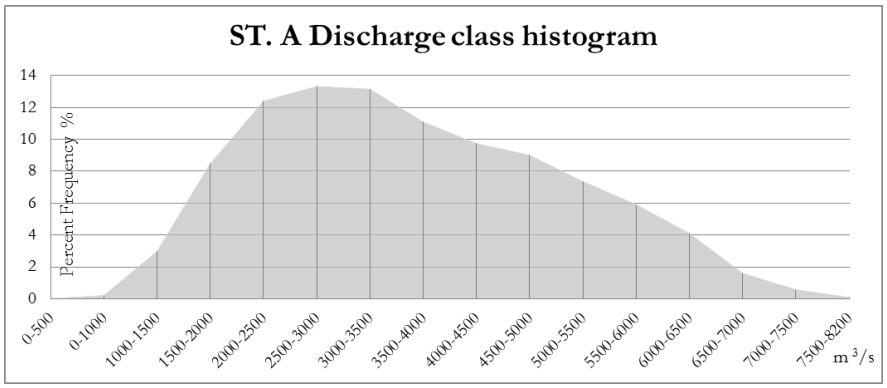

Q Class ID	Q Range (m3/s)	Freq. %
0	0-500	0.0
1	0-1000	0.2
2	1000-1500	3.0
3	1500-2000	8.5
4	2000-2500	12.4
5	2500-3000	13.3
6	3000-3500	13.2
7	3500-4000	11.1
8	4000-4500	9.7
9	4500-5000	9.0
10	5000-5500	7.4
11	5500-6000	5.9
12	6000-6500	4.1
13	6500-7000	1.6
14	7000-7500	0.6
15	7500-8200	0.1

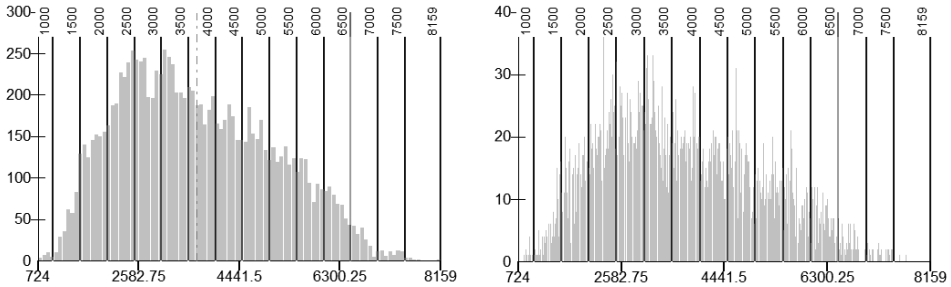

Figure 14. Discharge histograms for Station A; classified in 15 classes and 100 & 999 columns.

The highlighted years from the high flow analysis were studied in detail. All the stations were plotted annually to observe their relation along different years. General consistency and hydrograph agreement was visually checked with satisfying results; time series on all the stations and years evaluated were consistent with each other, in the sense that proportional relations were maintained. An important relation to have in mind which is later used to calibrate river flow partition is the discharge on the main and second branch which are registered on stations 2 and 3. These two branches hold the water that flowed together through Station A and later diverted. The relation changes a little in time and has no pattern with high or low flows, which raises an issue to investigate further.

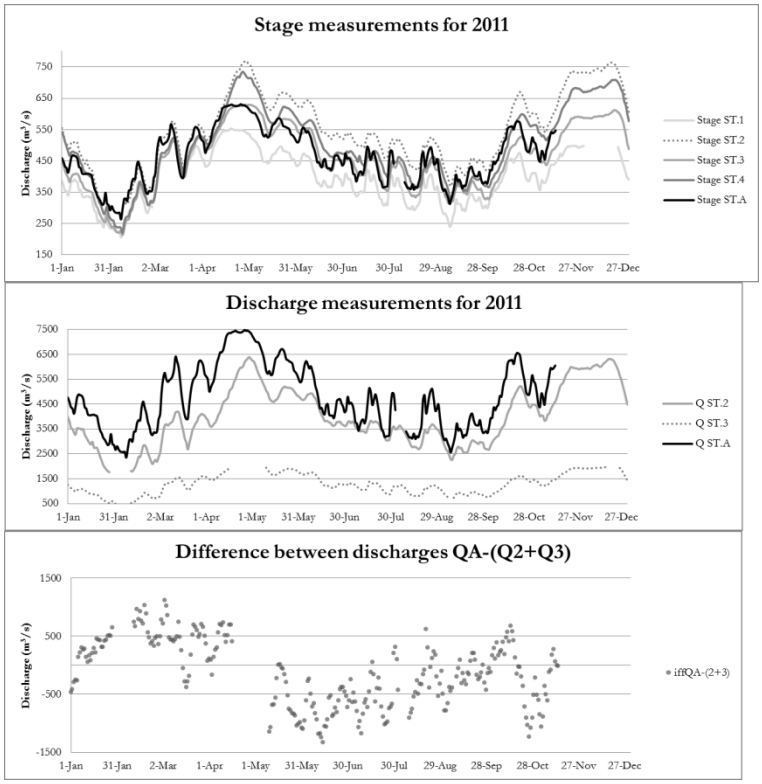

Figure 15. Measured data and relations for the year 2011.

The stage discharge relations (Figure 16) were also visualized and analysed for further use to calibrate the cross section's geometry. Initially the cloud of points had considerable variability, but it is found that the stage discharge relation maintains stable for some years, and suddenly another group of years maintain another relation, responsible for such variability. Years were analysed and grouped according to their stage discharge relation (Figure 31), relations later used for river simulation calibration.

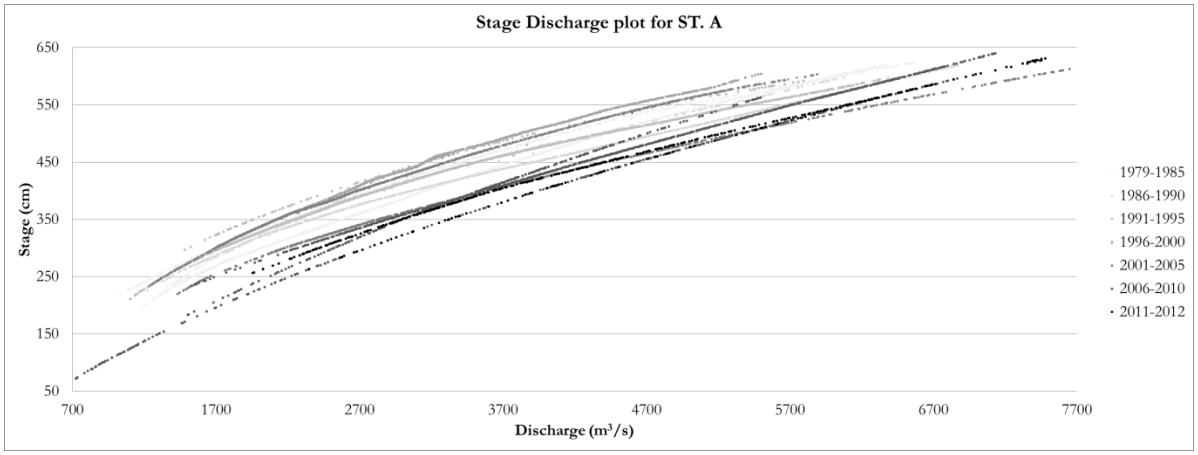

Figure 16. Stage Discharge plot for Station A.

5.1.2. Return periods of high flow events

The high flow events and return period analysis was done on the discharge and stage data, but only the results relating to discharge are shown (Figure 17). It is considered the stage data has too much variance that that have effect on the time series and eventual extreme event analysis. For example for a discharge of 3000 m3/s the total time series shows that stage could be around 3 to 4.5 meters. Te Linde et al., (2010)

and Alfonso (2010), also find that morphological changes manifest in the stage discharge relation. Together with morphological changes, climatic changes pose a challenge to include in hydrodynamic modelling.

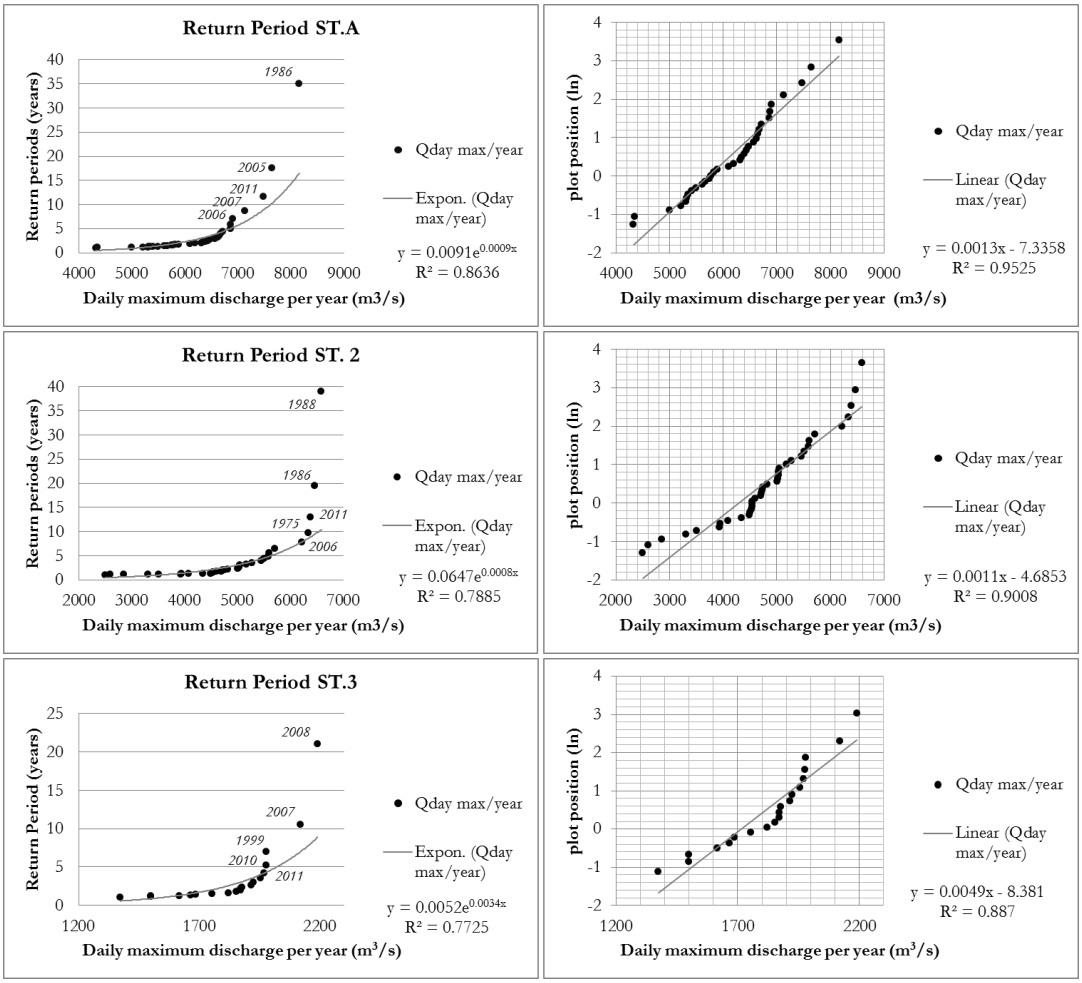

Figure 17. Return periods based on extreme events, Gumbel plots for Stations A, 2 & 3.

High flow discharges like in the year 1986 (Figure 18) or missing values like in 2010, affect the result of the return period analysis. For example if the 2010 series would be complete, it might have had the maximum historical discharge, changing the rank order and return period. The high flow years were plotted to aid also the search and selection of satellite images to capture the flooding events.

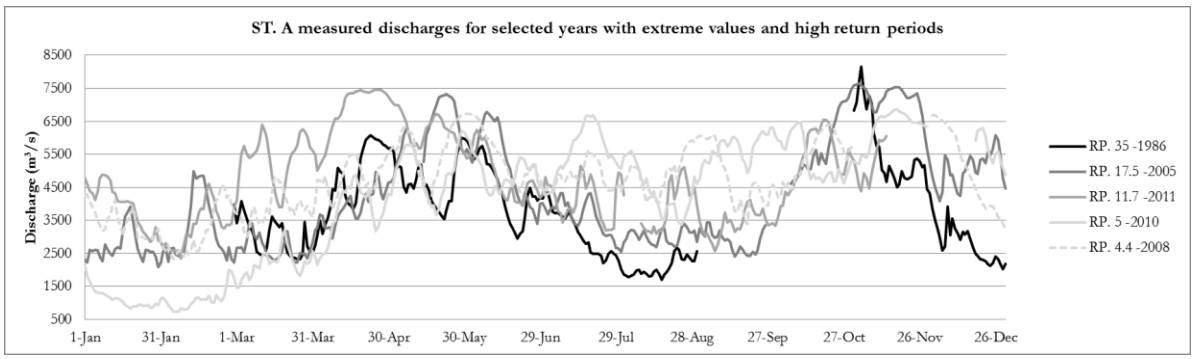

Figure 18. Measured discharge on Station A, for selected years with extreme values.

5.1.3. Linking imagery to river stage and flow conditions

The top ten maximum day discharge for each calendar year of the time series are identified with the return period analysis (Table 4). These dates give then the base to search for flood evidences in the satellite imagery. The following high flows were located in the daily time series and searched in the Landsat data base. Observing the peak for the first place, 1986 (Figure 18), it could possibly be an error. For that date the floodplain looks flooded on a cloudy image, but the extent is not the largest compared to other observations. The second year in rank is 2005 which is captured by two images on the 2nd and 18th of December. The events for 2008 and 2011 are clearly visible and captured at high flows.

Table 4. Top ten return period ranks for the discharge series, Stations A, 2 & 3.

		Discharge	Return			Discharge	Return			Discharge	Return
rank	year	ST.A (m3/s)	Period	rank	year	ST.2 (m3/s)	Period	rank	year	ST.3 (m3/s)	Period
1	1986	8159	35.0	1	1988	6590	39.0	1	2008	2190	21.0
2	2005	7650	17.5	2	1986	6466	19.5	2	2007	2120	10.5
3	2011	7480	11.7	3	2011	6390	13.0	3	1999	1979	7.0
4	2007	7132	8.8	4	1975	6344	9.8	4	2010	1978	5.3
5	2006	6907	7.0	5	2006	6224	7.8	5	2011	1970	4.2
6	1988	6873	5.8	6	1989	5710	6.5	6	2005	1956	3.5
7	2010	6867	5.0	7	2004	5608	5.6	7	2006	1925	3.0
8	2008	6714	4.4	8	1982	5590	4.9	8	1993	1916	2.6
9	2004	6672	3.9	9	2010	5512	4.3	9	2012	1878	2.3
10	2012	6649	3.5	10	1981	5460	3.9	10	2002	1872	2.1

5.1.4. River branches and flow partitions

The river partition could be observed from the discharge series. Taking into account that the water that passes through station A, diverts between the main branch and the second, and stations 2 and 3 are in each one, this became an objective for cross section calibration. The cross section arrangement around the connection nodes, determined how the water flow divided between branches. In the following table (Table 5) is a set of results on nine check points along the river. Check points 2 and 3 are on gauges 2 and 3. Check point station 5 is at the upstream and 9 at the downstream stretched, where the total mass of water is consistent.

Table 5. Simulated river flow branching percentages on 9 check points.

Test SET UP /0.025 n	*%*								
Discharge inflow (m^3/s)	*1*	*2*	*3*	*4*	*5*	*6*	*7*	*8*	*9*
1000	76	70	30	61	100	24	6	9	100
2500	76	69	31	60	100	24	7	9	100
5000	76	68	32	60	100	24	8	9	100
7000	76	68	32	60	100	24	8	9	100

Metadata on the river monitoring and calibrating system is not available, it is only known the is based on visual measuring based on fixed scales that measure water levels which are used to calculate discharge. No information about the cross section or calibration curves is available for any period. This situation raises the uncertainty of the river measurements which have a relative validity and can't be related to a datum.

5.2. Land cover

From the land cover analysis, information in two general lines was obtained; first focusing on the river, water bodies, flood extent and activity. The second deals in general land cover surface roughness for overland flow parameterization. Result can be outlined as follows:

Water & flood maps

1. Flood extent boundaries, with date context.
2. "Normal" water bodies.
3. Breaches, overtopping and flood activity identification, location and dating.
4. River network and dimensions (base 1D).
5. River dynamics (changing cross sections).

Land cover maps

1. Land cover (vegetation) recognition and map. Application for cross section location.
2. General units to parameterize surface roughness for 2D model input.
3. Dense and tall vegetated patched for DEM offset identification and evaluation.

5.2.1. Water & flood maps

Water and flood maps were produced for different extreme events identified from the river gauge data and known flood occurrences. Even though water bodies are dynamic, a "normal" extent can be established for later use when quantifying flooding areas, as water bodies should to be discounted. The normal water bodies obtained from a previous work gave almost the same results as the classification of January 29 2001 (Figure 19). Including the river surface, water bodies cover 32239 pixels of 270 meters. Around 40% are river pixels based on the count of 12400 for branches 1 and 2. For the area both layers share, the total number of pixels classified (23686) coincide in 63%. The remaining percentage is shared 20 % and 17% where the higher percentage corresponds to water pixels from the composite image that are not captured by the water map of January 29, 2001. 17% were pixels classified as water in 2001 and not captured in the composite map. The differences are concentrated around the shorelines, for it is evidenced that few images do not capture the complete movements or dynamics the water bodies have in the study area.

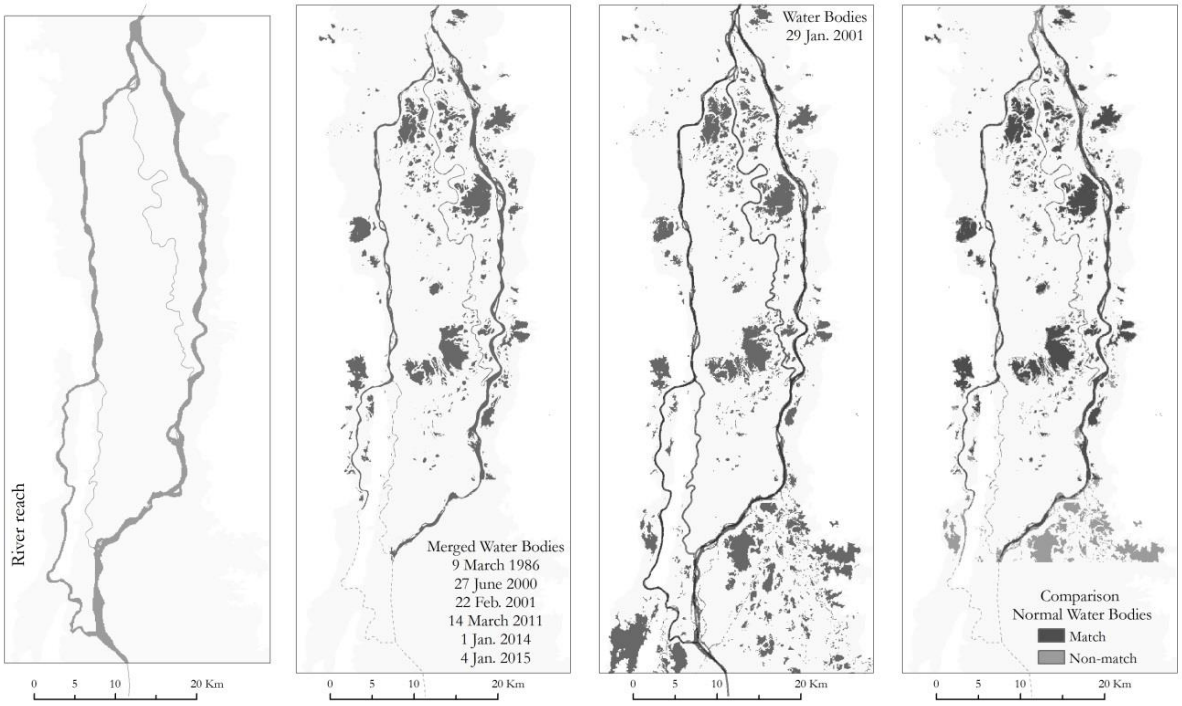

Figure 19. Normal water bodies results and contrast.

Flood extents for December 2005, June 2006, December 2008 and a rising flood on March 2011 were classified (Figure 20). A visual interpretation was done on several cloudy images for the peak of 2011. Floods have a different spatial expression and are not completely dependent on the river flow. Much more factors determine floods from happening. Some general patterns can be observed with the spatial analysis of the floods maps and are consistent with the simulation results.

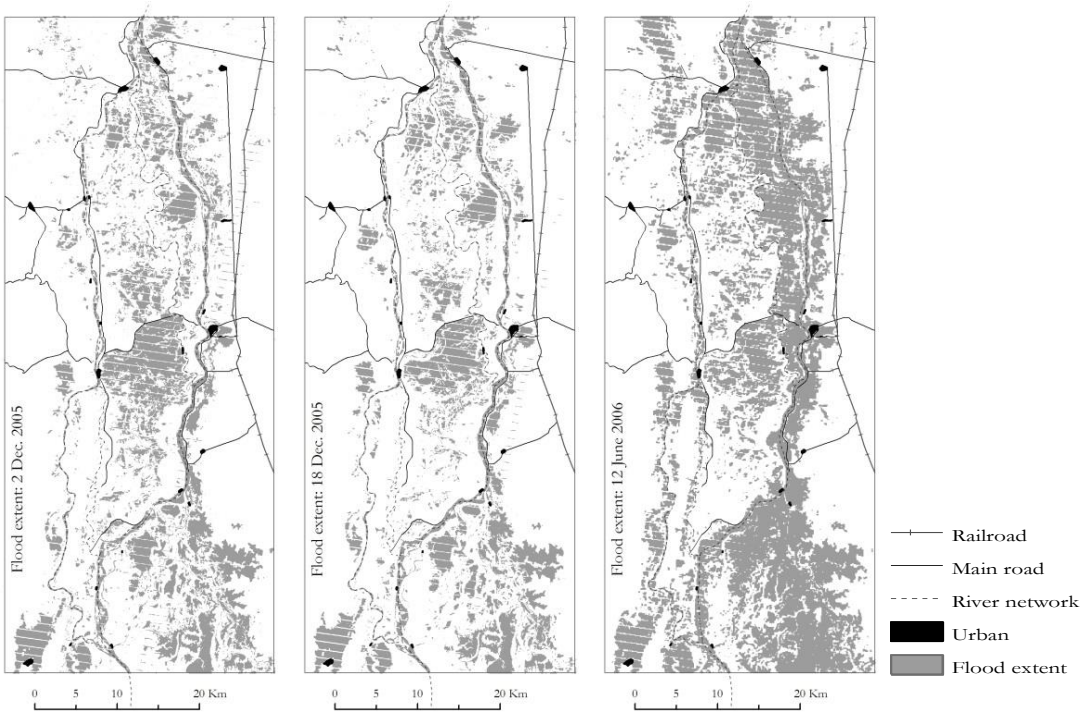

Figure 20a. Flood maps for December 2 and 18 2005 and 12 June 2006.

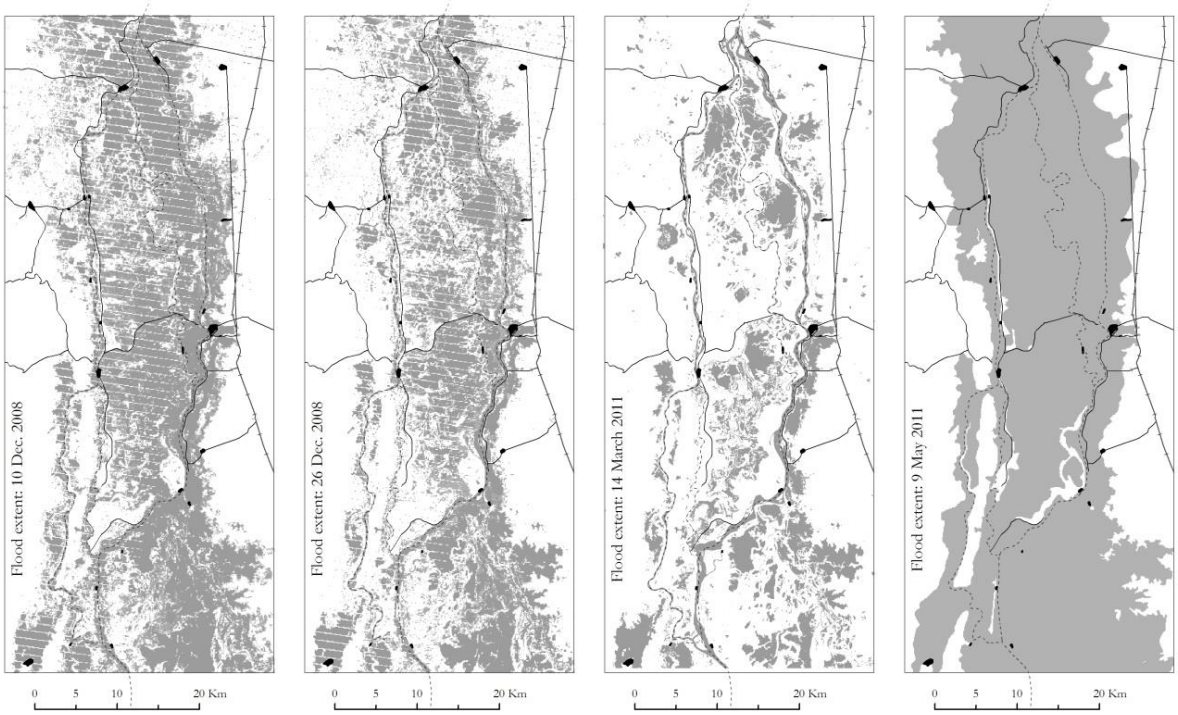

Figure 20. Flood maps for 2005, 2006, 2008 and 2011.

An additional testing was done to check the effect of mapping methods. From the maximum observed extents, the classified for 2008 and interpreted extent for 2011 were compared (Figure 21), additionally the water bodies are overlaid to observe the flood extent beyond what is covered by water already. From a total of 190854 classified pixels, both layers coincide in 70% coincidence or match, where the flood extent was mapped for both of the dates. The remaining 30% is between the flood that was only mapped for 2008 on 3% of the total observed flood extent and 27% of the pixels were only mapped for the 2011 extent.

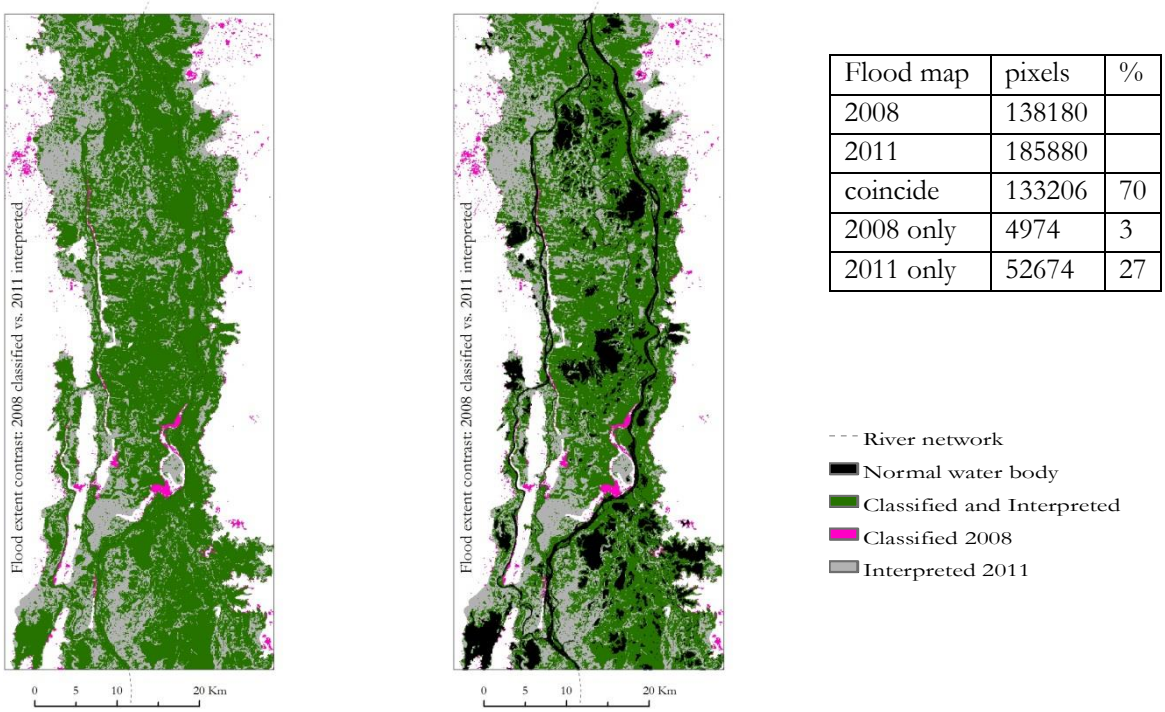

Flood map	pixels	%
2008	138180	
2011	185880	
coincide	133206	70
2008 only	4974	3
2011 only	52674	27

Figure 21. Contrasting flood classification December 2008 and flood interpretation May 2011.

With the Landsat time series, permanent and other observed breach points were located (Figure 22). Overtopping is depends more on interpretation to establish. Permanent communications exist from the river to the lower east wetlands, and also from these wetland complex to the river where two or three locations are visible, on high flows they become one communication area. On the road that goes from (Morales-Gamarra) west to east in the middle section of the AOI, there are three breach points that appear on rising waters. The road built across the floodplain on a natural dike, blocked natural flow paths with south-north direction.

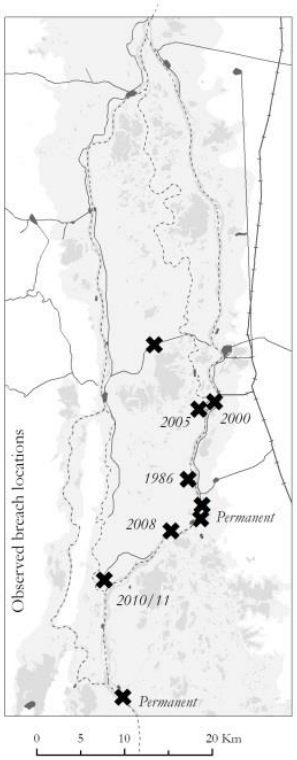

Figure 22. Location of observed breach points.

MODIS imagery verifies and supports the findings with Landsat imagery. On peak and flood events the patterns match while in normal moments, like the one shown below (Figure 23) in January of 2010, the water bodies are consistent with the classified ones. The first image of 2007 is in rising level moments with no breach point while in the image on the 21st the breach point is visible like in the Landsat images and an important breach point in the flood simulations.

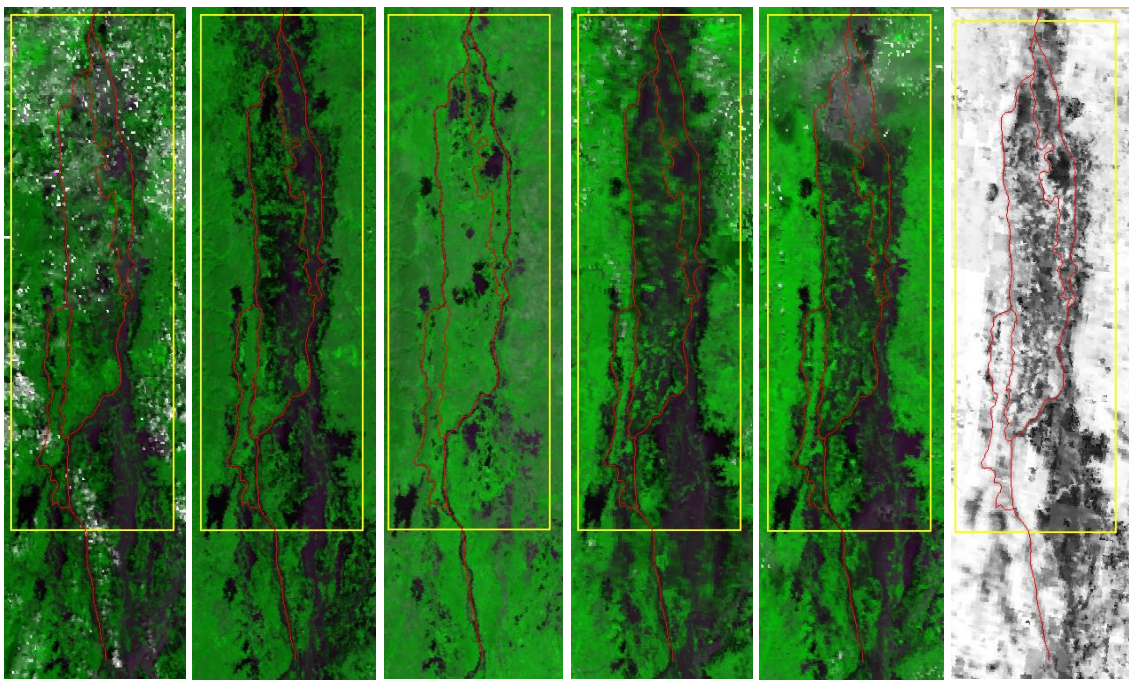

Figure 23. Left to right; MODIS 9Q1, December 4 and 21 2008, January 27 2010, May 4 and June 6 2011. NDVI product 13Q1 May 9 2011.

5.2.2. Land cover maps

Besides the focus on water units, general land cover had to be mapped to parameterize the surface roughness for overland flow, as an input for the 2D model schematization.

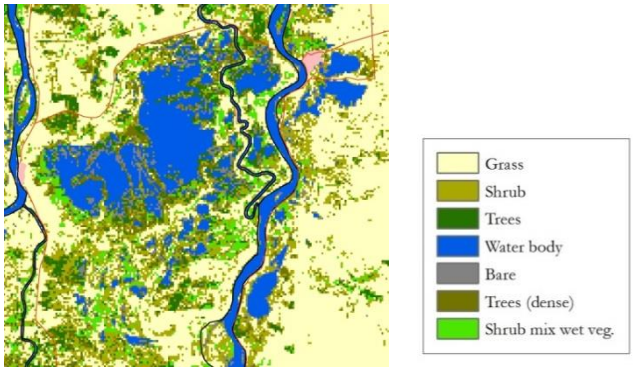

Land cover	LC code	Manning's coefficient	Friction description
Grass	1	0.025	Low
Shrub	2	0.05	High
Trees	3	0.03	Medium
Water body	4	0.001	No friction
Bare	5	0.02	Lower
Trees (dense)	6	0.04	Medium
Shrub mix wet veg.	7	0.05	High
Urban	8	0.035	Medium

Figure 24. Surface roughness parameterization from land cover units.

The friction N value or Manning's resistance to flow values are assigned to the land cover units of the study area as listed in the table above (Figure 24). Landcover classes are originally at 30x30 meter/pixel and were resampled to 92.4 and 270 meter/pixel resolution for the respective 2D inputs.

Vegetation is in permanent change, inducing potentially high requirements for this parameter. Also during flood events fiction values vary with the advance, increment and recession of the flood. A general representation fulfills the model input requirement and can be further explored. As this parametrization depends on the land cover representation, different kinds of land cover maps will have result in different distributions of friction values. At the same time the way of assigning or source of friction value will also have consequences on the final parameter distribution. Water bodies for example are differentiated only with a very low friction value.

5.3. Topography; elevation model

From the work with the elevation data two main model inputs are derived. The SRTM elevation is base for the bank elevation of the cross sections for the 1D river schematization. A modified elevation grid is input for the 2D surface for overland flow simulations. While extracting the bank elevation data, elevation offsets that coincided vegetation block were found. Accounting for the variability of elevation and land covers was done. Also elevation was related with the maximum flooding extent observing their relation.

5.3.1. DEM quality assessment

The SRTM gave a good match when contrasting with the IGAC geodetic points for the neighbourhood of the study area (Figure 25). Differences between the two sets based on 24 point have an average of -0.2 with standard deviation of 2.5, only accounting positive values the average is 1.8 with standard deviation of 1.7. Ten results are below 1 meter and only two points differ for more than 4 meters, one 4.5 and the greatest difference of 7.1 meters in the hilly area at the south. There was no pattern identifiable with land cover or general land form to have effect on the difference between these two elevation sets. One data set is not always greater or lower than the other; differences seem random and could be attributed more to the variability and accuracy of the SRTM DEM on describing terrain elevation.

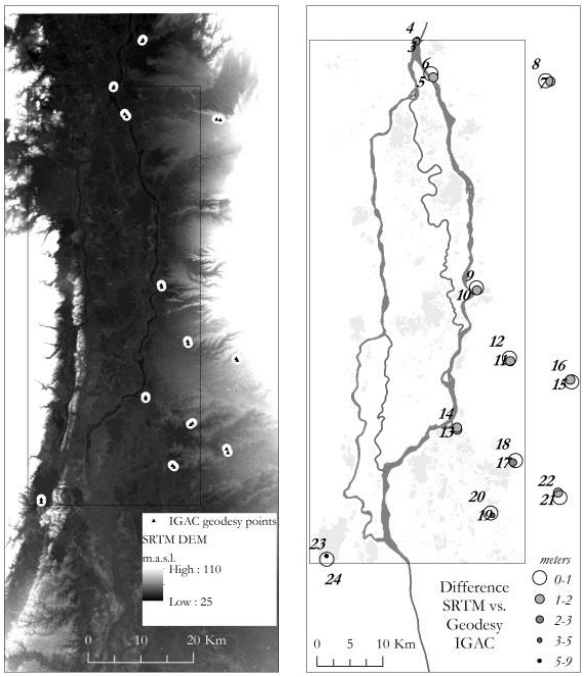

Point	Land form	Land cover	IGAC Z	SRTM Z	D_Z
1	terr. hills	road grass bush	37.08	40	2.9
2	terr. hills	road grass bush	32.94	36	3.1
3	floodplain	urban	32.51	37	4.5
4	floodplain	urban	32.68	36	3.3
5	floodplain	urban	33.71	34	0.3
6	floodplain	urban	33.40	35	1.6
7	terrace	road	86.50	87	0.5
8	terrace	road	84.43	84	-0.4
9	floodplain	urban	43.69	44	0.3
10	floodplain	urban	45.56	44	-1.6
11	hills	road	53.97	51	-3.0
12	hills	road	56.32	56	-0.3
13	floodplain	urban	43.80	45	1.2
14	floodplain	urban	44.24	44	-0.2
15	hills	road	101.86	102	0.1
16	hills	road	104.57	104	-0.6
17	terr. hills	road urban	45.46	47	1.5
18	terr. hills	road	50.22	49	-1.2
19	terr. hills	urban	48.94	45	-3.9
20	terr. hills	urban	46.18	46	-0.2
21	terrace	road trees	61.62	60	-1.6
22	terrace	road grass	62.63	62	-0.6
23	terr. hills	urban	60.15	53	-7.1
24	terr. hills	urban	55.58	53	-2.6

Figure 25. IGAC geodesy control points vs. SRTM elevation contrast.

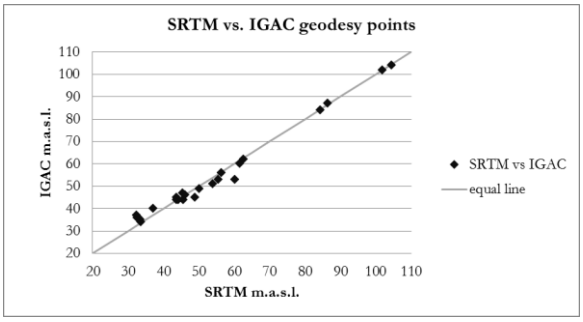

Figure 26. Scatter plot contrasting SRTM elevations with IGAC geodesy control points.

The observed variance or variability of SRTM elevation on clear flat patches was higher than expected and can be seen in 5.3.4.

5.3.2. DEM as base for cross section bank elevation in river 1D schematization

The measured cross sections were analysed and decided not to use because of their variation between themselves and when compared to the bank elevation on the SRTM. As it is described in the methodology, 24 locations were selected in combination with Landsat data, to extract the values attempting to avoid locations with dense vegetation inducing more error. Observing the slope of the final channel and the general performance of the 1D simulation, it is considered that the SRTM offers an advantageous source of topography when data is scares.

5.3.3. DEM as surface in 2D flood simulations

Corrections for surface flow were seen in literature but do not apply for this case, as an objective was to assess how does overland flow transits on the SRTM surface in the flood model. Forcing a flow path would bias this analysis. Corrections along the main river were done to match an homogeneous bank elevation instead of a river depth or surface. Corrections on vegetation were considered but time was not enough.

Correction upon the river network can be seen on the right Figure 27. Only branches 1 & 2 are wide enough to be captured in the CGIAR SRTM DEM (left). The river filled elevations in the CGIAR product (center) created problems in the 1D2D simulations, as they were representing a pit under the schematized river. DEM elevations below the river were given a smooth bank elevation, matching the 1D design (right).

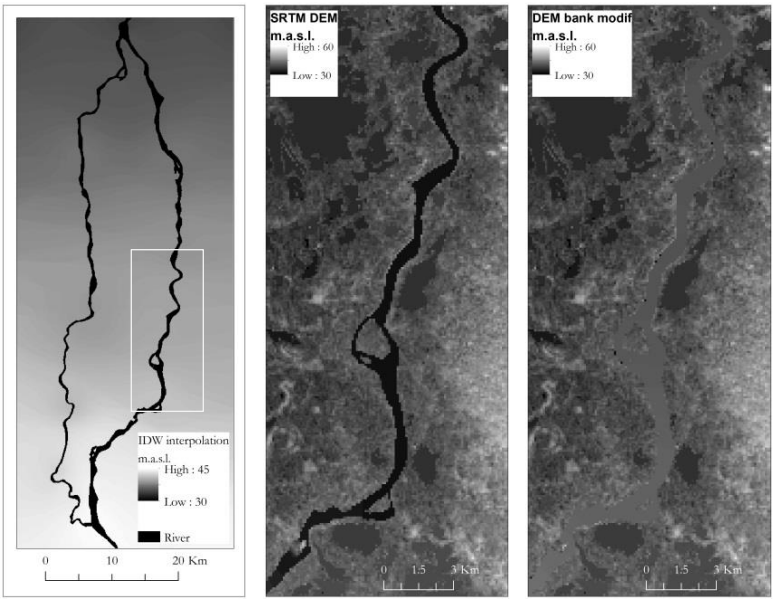

Figure 27. River bank elevation modification on the SRTM DEM.

Once the accepted DEM on original resolution was ready, it was resampled to the trial resolution of 270 meters per pixel. A previous test was done on 300 meter resolution and below the differences from the resampled to the original elevations can be seen (Figure 28).

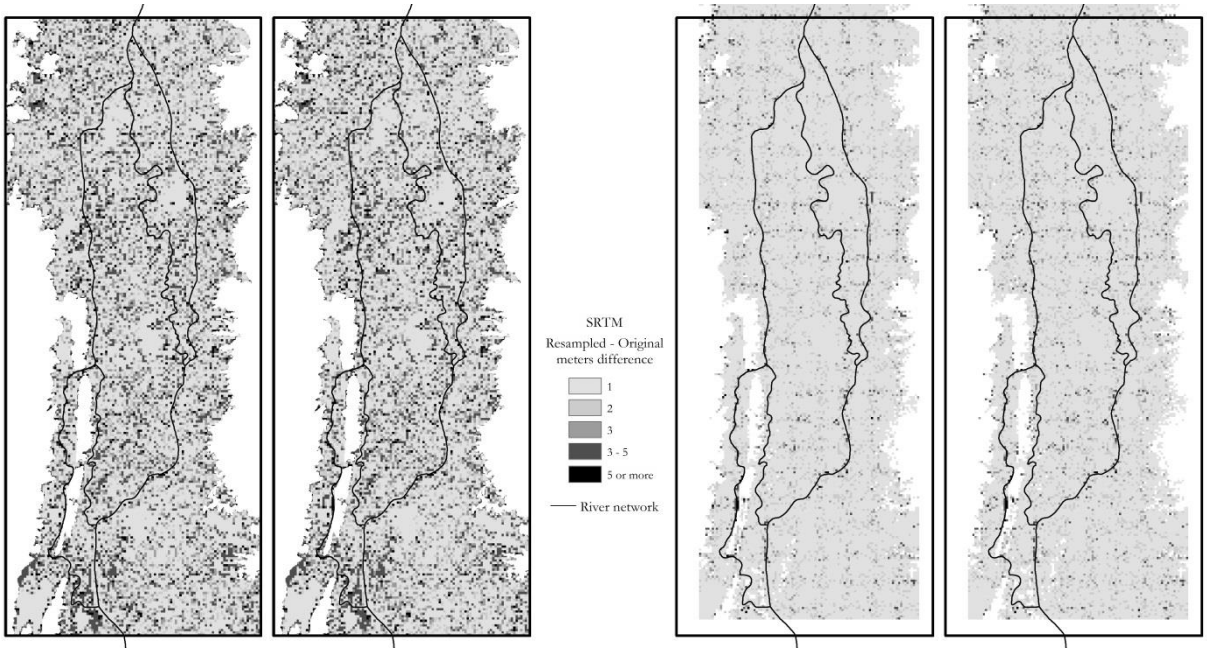

Figure 28. SRTM90m – Rsmpl_300m Nearest Neighbor (far left), SRTM90 – Rsmpl_300m Cubic Convolution (left), Rsmpl_270m Bilinear – SRTM90m (right) and Rsmpl_270m Cubic Convolution – SRTM90m (far right).

Resampling the original DEM to pixels of 300 and 270 meters was done with better results on 270 m. When comparing to the original DEM, larger differences were observed on higher elevations. Masking out terrain with elevation above 50 masl, the difference between the resampled and original DEM was evaluated. For the 270 meter resample, the best results were obtained with cubic convolution, with mean difference of 0.0079 and standard deviation of 0.9. For the bilinear method, 0.049 mean difference and standard deviation of 1.0. For cubic convolution the results ranged between -10 and 8, and for bilinear

interpolation the range was wider, from -8 to 25. The grid resulting from the cubic convolution resampling to 270x270 meter/pixel was chosen as input for the 2D surface.

The river bank elevations from the cross sections were interpolated to produce an elevation map for the river. As the elevations within the river are taken care in the 1D operations, there is no need to burn in the bathymetry or cross section profile in the 2D grid. GIS work was done to produce a river bank elevation map and change the elevations of the original DEM before resampling.

5.3.4. Vegetation offset evidence

Inside study area two cases of clear elevation offsets are found, one in the south where the near breach point in 2011 flood made way, and another near to the center on a natural flooding forest. Outside study area there is one clear case, where several blocks of oil palm plantation raise around clear cut grass plots. The DEM does not capture the true elevation of the canopy, but does create an offset of around five to ten meters (Annex 2). For example (Figure 29) tree patch 2 and grass patch 1 should have similar elevation as well as tree patch 5 and grass patch 2. This fact makes it more challenging to get rid of the vegetation effect, making not applicable corrections based on just field measurements on canopy heights. This is still a line of work and research with radar interferometry and vegetation backscatter.

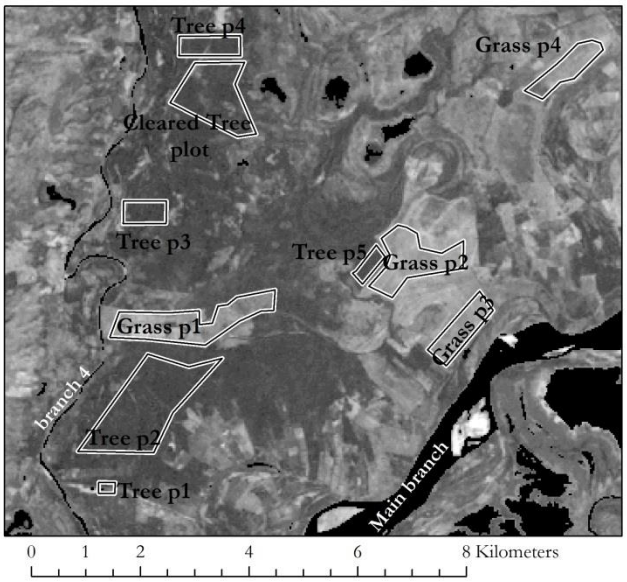

Figure 29. Location of samples to evaluate DEM elevation, over Landsat ETM band 29/01/2001.

5.3.5. Elevation slice maps

Can topography itself be enough to map flooding areas and flood extents? Topography can serve as a general indicator of flooding boundaries or maximum elevations as bound line and not explain in detail flood prone zones. For the study area the elevation of 45 m.a.s.l. gives a good indication on the boundary in the upstream region (Figure 30), where also there is more geological control like on the southern west region of the AOI where there are hills present rising inside and giving boundary to the floodplain. Towards the north and also eastern side, elevation loses capacity to describe floodable areas. In general it can be said that for the AOI flood does not occur above 50 m.a.s.l. and that elevation mask is useful to define an area to contextualize the results in terms of area (ha). It is also useful to clean the flood map classifications where errors are produced outside the floodplain from shadows, tributaries and vegetation that are not focus of the analysis.

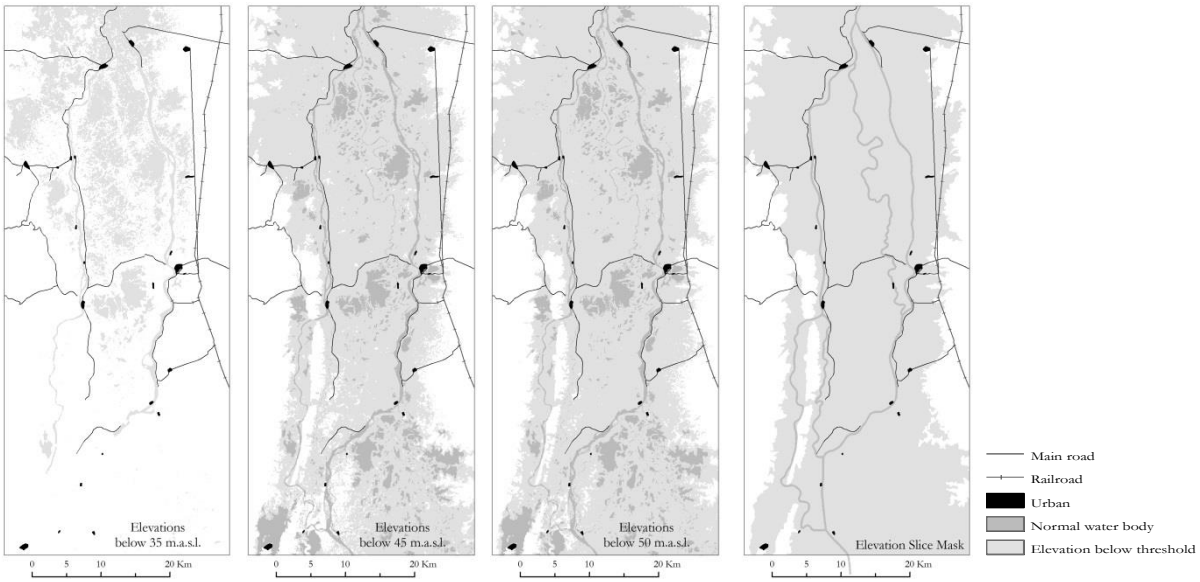

Figure 30. Elevation slice maps (35, 45 and 50 m.a.s.l.) and mask, center include normal water bodies.

5.4. 1D2D flood modelling

The final flood model results as its construction are divided between the 1D and 2D parts. The channel set up took considerable testing on different setups. Even though surface roughness is determinant on surface flow and even overbanking locations, having effect on the flood extent simulations, flood extent it is considered greatly a consequence of the 1D river system functioning. Agreement with real terrain conditions must be achieved with later field measuring and monitoring efforts. A full sensitivity analysis could not be done due to time constrains and long modelling time for simulations. For final presentation purposes of the model in construction, contrast between two or three results with different set ups and parameter variation is done.

5.4.1. 1D simulation results

As it was observed in the Stage Discharge analysis, relations only hold for some years until calibration is done and subsequent number of years the same happens. In Figure 31, it can be seen how records from 1999-2002 align, while 2006-2008 and 2010-2011 present another relation. When the cross sections are synthesized, the relation between the real geometry and possibility to reproduce the observed Stage and Discharges is lost.

For calibration, the stage discharge relations were used to find a reasonable cross section design setup for the 1D river network. Numerous simulations and setups were tested (Figure 31), combining slight changes in Manning's friction coefficient. A satisfying setup was selected and maintained through the 1D2D simulation runs.

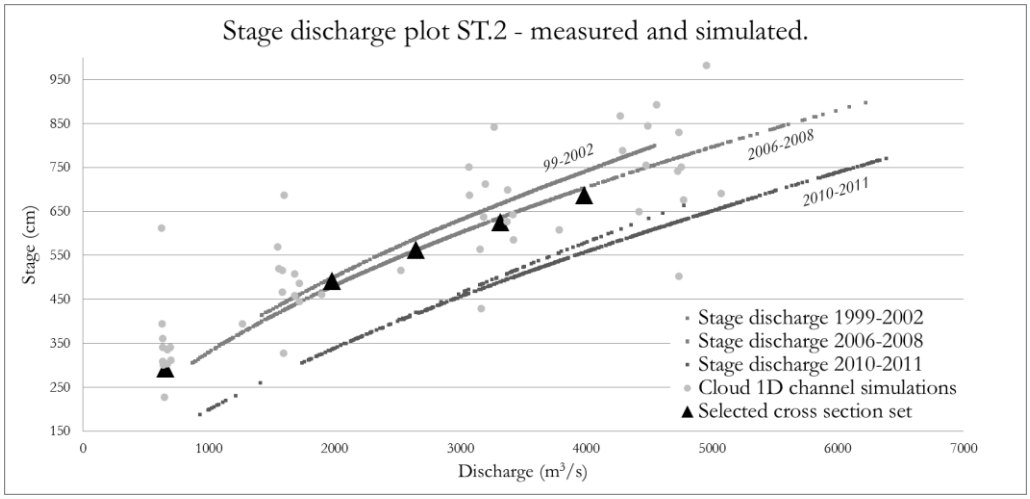

Figure 31. Stage discharge plot for Station 2, measured and simulated data.

As the observed river stages revealed that peaks in the stations upstream appeared the next day at stations downstream, this lag was used to calibrate the Manning friction vale (Figure 32). Runs were done with increasing values starting at 0.01 until 0.05, and best results with 0.025. Value of 0.03 results in better timing but causes overtopping too soon.

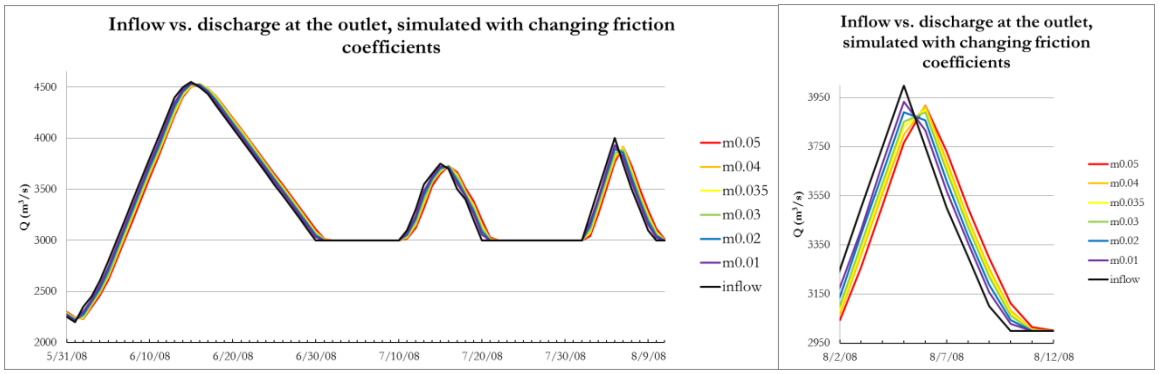

Figure 32. Simulated discharge with changing friction values.

Once the cross section geometry was accepted to continue and the surface roughness selected, as a validation trial the complete year of 2010 was run on 1D Figure 33). For station 2 the stage is rather similar being slightly overestimated and underestimating the discharge. For station 3, stage is considerably overestimated and river discharge slightly overestimated, with more offset at the peaks. The general hydrograph pattern is coinciding.

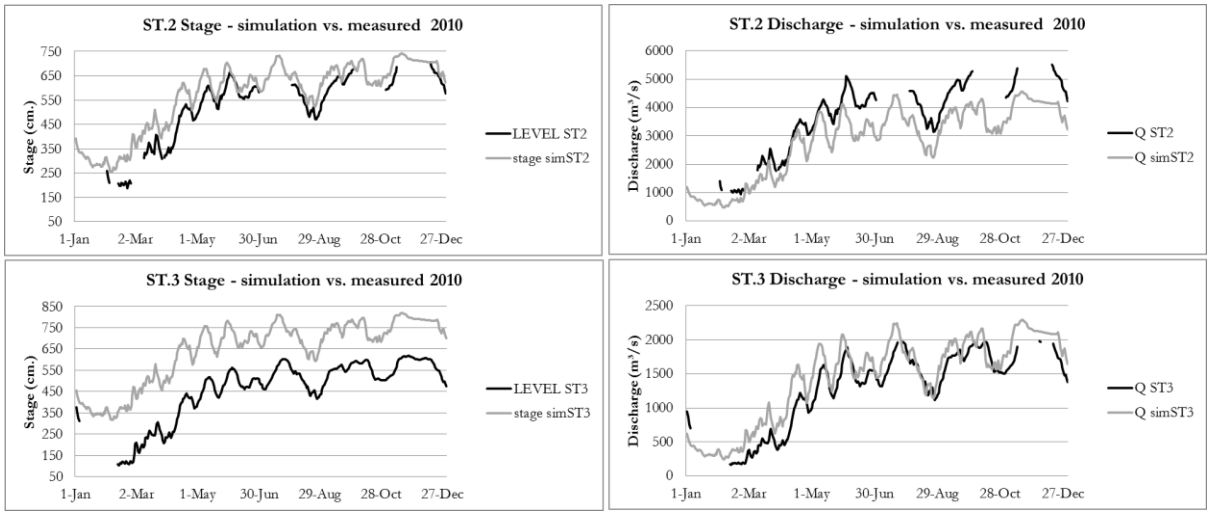

Figure 33. 1D Stage and discharge simulation results for Stations 2 & 3.

As 1D simulation does not loose water from the channel, a 1D analysis is done again on the 1D2D run of 2011 (Jan. 01 - May 31) and is presented as part of the results in the next section (Figure 35).

5.4.2. 2D simulation results

Preliminary flood simulations

The first simulations of the complete study area on general resolution (270x270 meter/pixel) were done on continuous flows with the unsteady mode setting. It was tried with the steady mode setting, but crashed because it did not reach the steady state. The friction coefficient was set homogeneous for the 2D grid and later was distributed based on general land cover for the final simulations.

From the flooding results on the continuous flows, it was observed that overtopping was happening before reaching channel capacity. A switch in the SOBEK 2D program settings, allows the use or not of embankments, and in this case the use of embankments forces the water inside the 1D channel until its full capacity. On the other hand without embankments, 1D channel can overtop as soon as the water level reaches the elevation of the surface pixel. That is another reason why it is advisable to produce a bank elevation map burned on the DEM.

Steady state discharges of 3000, 3500 and 4500 m^3/s were set as inflow boundaries for 30 and 45 days with the embankment option turned off in the 2D module setup. Simulations were run with and without the embankments setting option. When off, the inflow was reduced by 2000 m^3/s to avoid exaggerated flooding, as the idea was to observe how they were happening with increasing discharge.

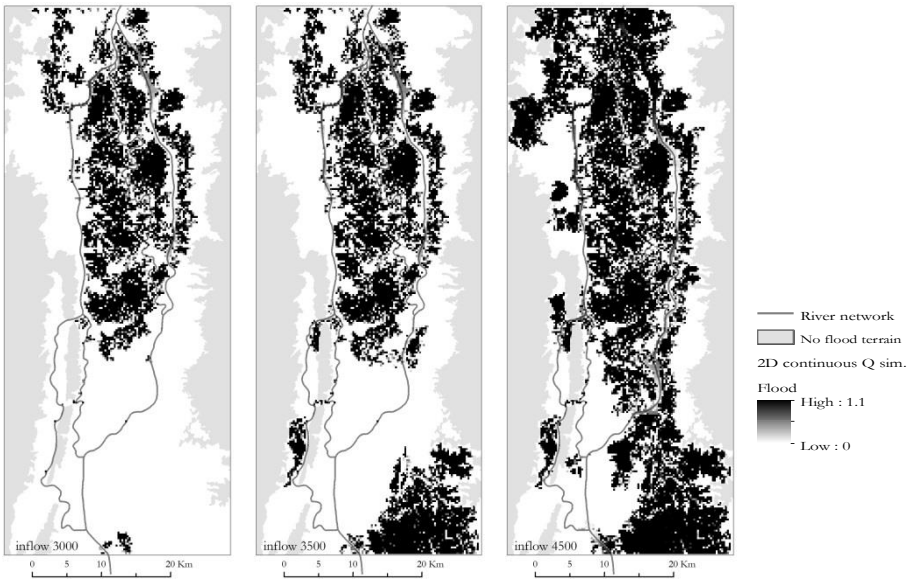

Figure 34. Flood simulation results with steady state inflows (left to right; 3000, 3500 and 4500 m^3/s).

The results of these simulations are already reveling interesting facts (Figure 34), like the flood path from branch 2 at the north east. In this point observed with the Landsat images, an open channel with the river of about 60 meter wide was cut off as a generalized practice to avoid flood problems and facilitate agricultural use. The filling of the wetland complex at the south east corner is also an interesting result that coincides with the observations in imagery on how the inflow from this area determines the flooding on its way north and to the right of the river. This flood pattern can be seen in numerous images and particularly on the 2006 and 2007 floods. In many other moments with no floods on rest of the study area, this zone is frequently flooded. Control and protection measures are also evident in the imagery, but the design seems not to account for the reality of that funneling area.

For the final simulations on 270x270 meter/pixel resolution, the inflow boundary was defined as the observed discharge at Station A for the first 5 months of 2011. For the 90 m resolution, the simulation lapse was of March to May 2011 due to computing capacity. For the first case the simulation took around 5-6 hours, while the final 90 meter simulation took 5 days to process.

The overland and channel simulation results are shown below (Figure 35). For the southern part of the central floodplain the 3 checkpoint stations show how the flood happened in those locations. Contrasting with the 1D simulation is useful to have a better picture of the event, observing when the overtopping happened and the effect on the remaining water in the channel. This fact is not represented in the sole 1D setup. After overtopping, the simulation peak diminished considerably compared to the gauge measurements at Station 2 as an example. There is no more water available to reach the measured peak as it has left the channel. An important inflow coming from the wetland complex in the south east corner is missing. Inflow at that point is an important trigger on high stages on that stretch of the river causing overtopping and breaching to the central floodplain. High stages determined by this wetland complex also give a back water effect on the river at this stretch where breaches are seen through time. One example is clearly resulting in the 2D simulations, where station check point st_iii was set. This point was breached in 2008, on 2011 the breach point was further south before the connection to branch 4, where a more dense bushy and arboreal vegetation is found. This vegetation results in a higher terrain representation and prevents occurrence of simulated floods on the south western side (limiting branch 4) of the central floodplain.

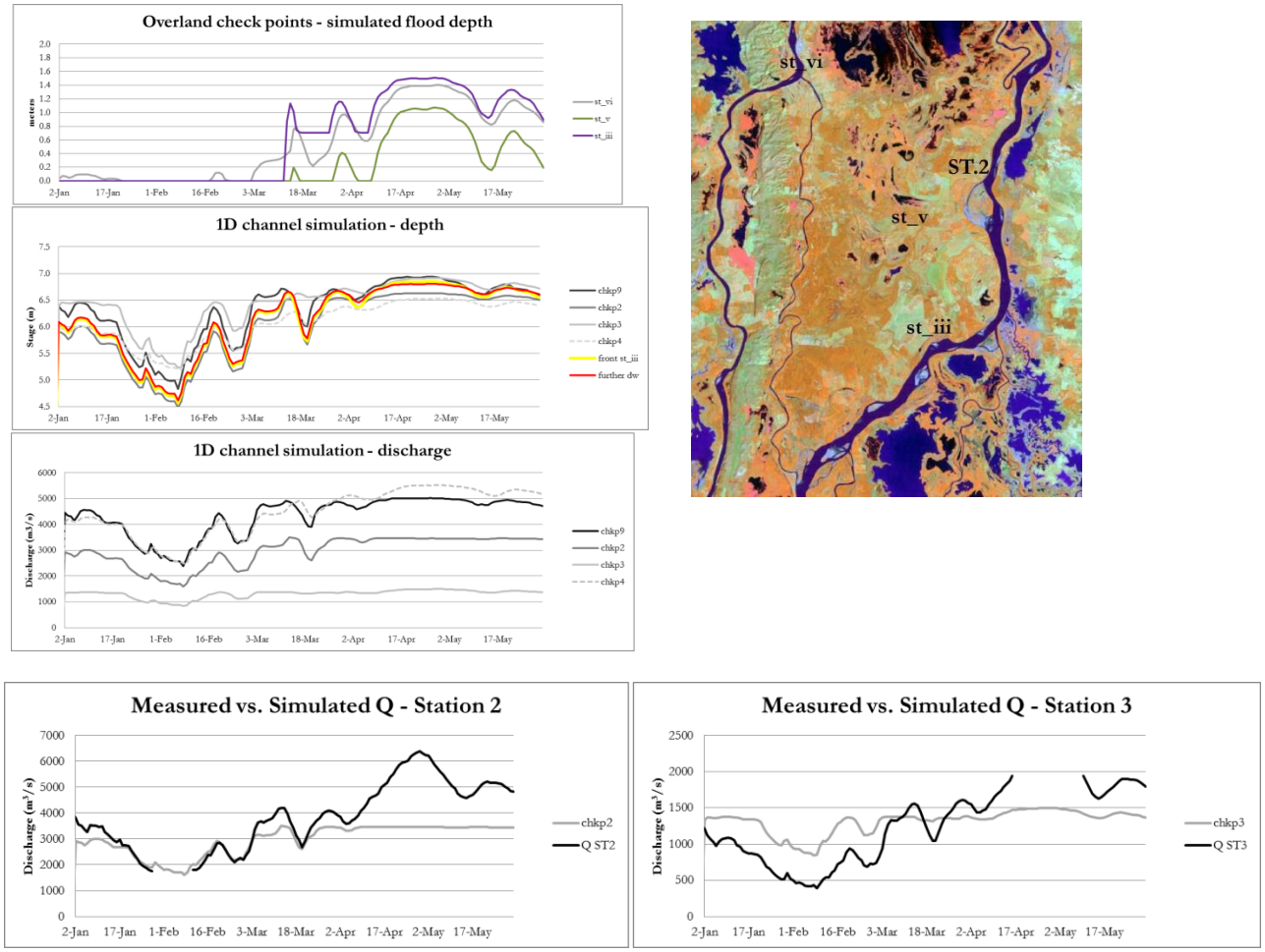

Figure 35. 1D2D simulation results with 270x270 meter/pixel resolution.

Final flood simulations

To have comparable results, simulations for the 270x270 meter/pixel were run again for three months matching the 90x90 meter/pixel simulation time. To assess the flood simulations, these were evaluated in several ways. Simulations were run with different upstream and downstream boundary conditions, and DEM spatial resolutions. Two event simulations are compared with the mapped flood extents. The first analysis was done comparing the maximum flood extents of the year 2005 and 2011. The second test was to compare the flood extents for the period of 2011 and raising the downstream boundary condition by 1.5 meters. The previous tests were done on spatial resolution of 270x270 meter/pixel. The third analysis was to compare the results of using spatial resolution of 90x90 meter/pixel for the calculation grid. The last two tests contrasted the observed or mapped flood events for 2005 and 2011 with the simulated ones.

Homogeneous and distributed roughness values

To observe the difference in the simulated flood extent when homogeneous or distributed surface roughness is applied, the following figure Figure 36) was prepared for two simulated and observed flood moments. March 14 is the 13th day in the simulation and shows how the flood stats to happen. The flood with distributed roughness has already advanced through the central floodplain while the case with homogeneous roughness is just has only flooded a small portion of the central part, where both coincide. Once the simulated flood advances in time, both resulting extents have a similar extent, differencing by just a 102 pixels.

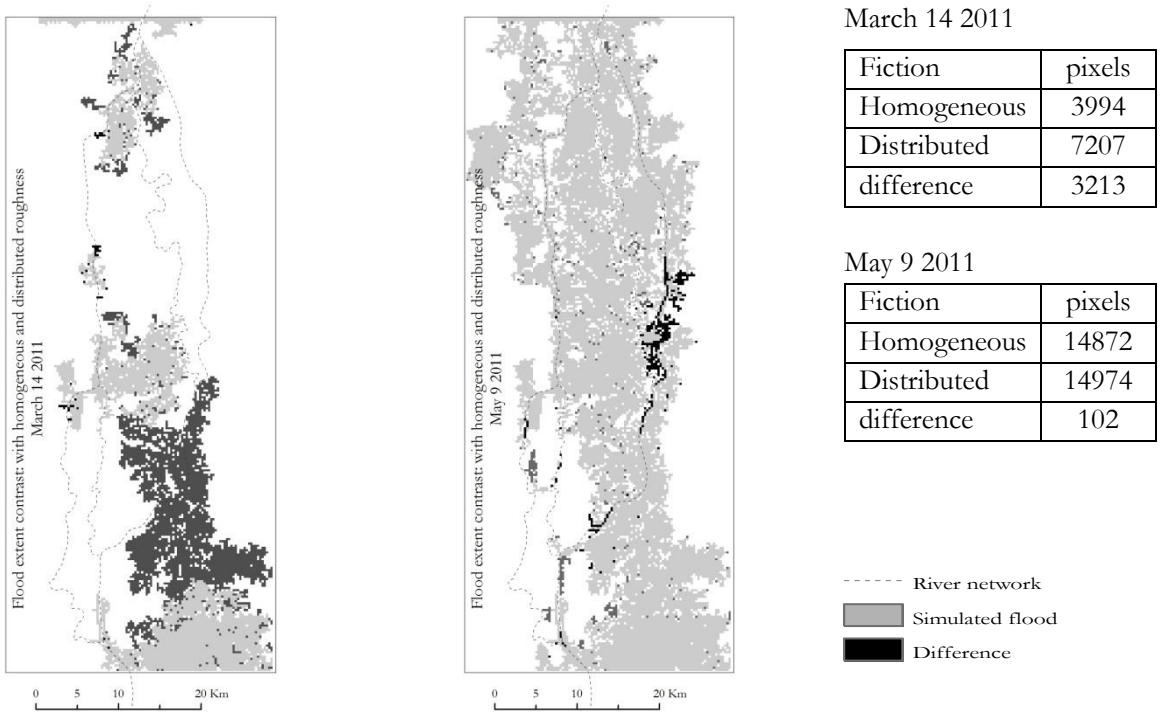

March 14 2011

Fiction	pixels
Homogeneous	3994
Distributed	7207
difference	3213

May 9 2011

Fiction	pixels
Homogeneous	14872
Distributed	14974
difference	102

Figure 36. Contrasting flood simulations with homogeneous and distributed friction values, for March 14 and May 9 2011.

Changing upstream boundary condition

From the high flow analysis it was observed that 2005 and 2011 had no gaps, being selected for simulation upstream boundary conditions. Their peak discharge only differs by 170 m^3/s. The simulated flood extents are almost equal, differencing by only 129 pixels, which can be seen dispersed in the study area (Figure 37), with a small grouping north where branch 3 diverts from the main branch.

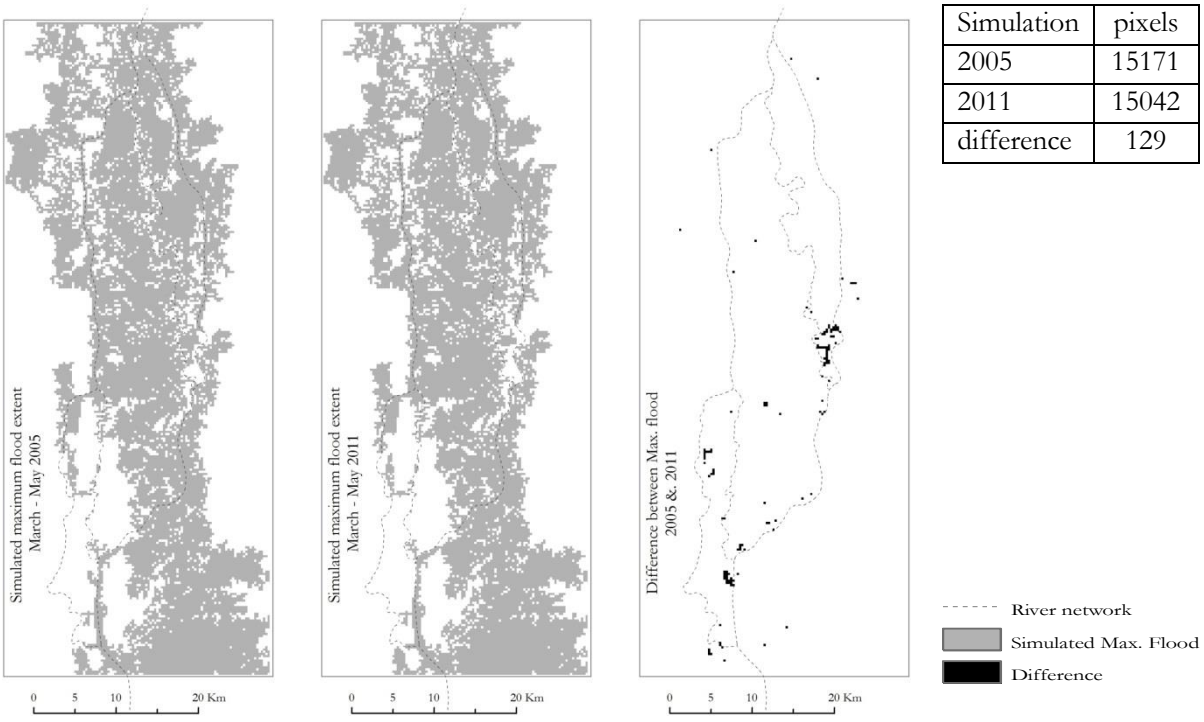

Simulation	pixels
2005	15171
2011	15042
difference	129

Figure 37. Contrasting flood simulations resulting from different inflow boundary conditions.

Raising downstream boundary condition

To assess the change the 2011 flood extent with changing hydraulic state of the boundary condition, this was raised by 1.5 meters and compared the results. First it was done for May 9 but the results were almost equal, so the comparison was held for March 14 2011. It is visible how it increases the extent of the flood in the downstream area by 342 pixels (Figure 38). The effect of the initial conditions can also be seen in in the first simulation steps where the back water effect created by the higher head makes a faster advancing flood wave upslope.

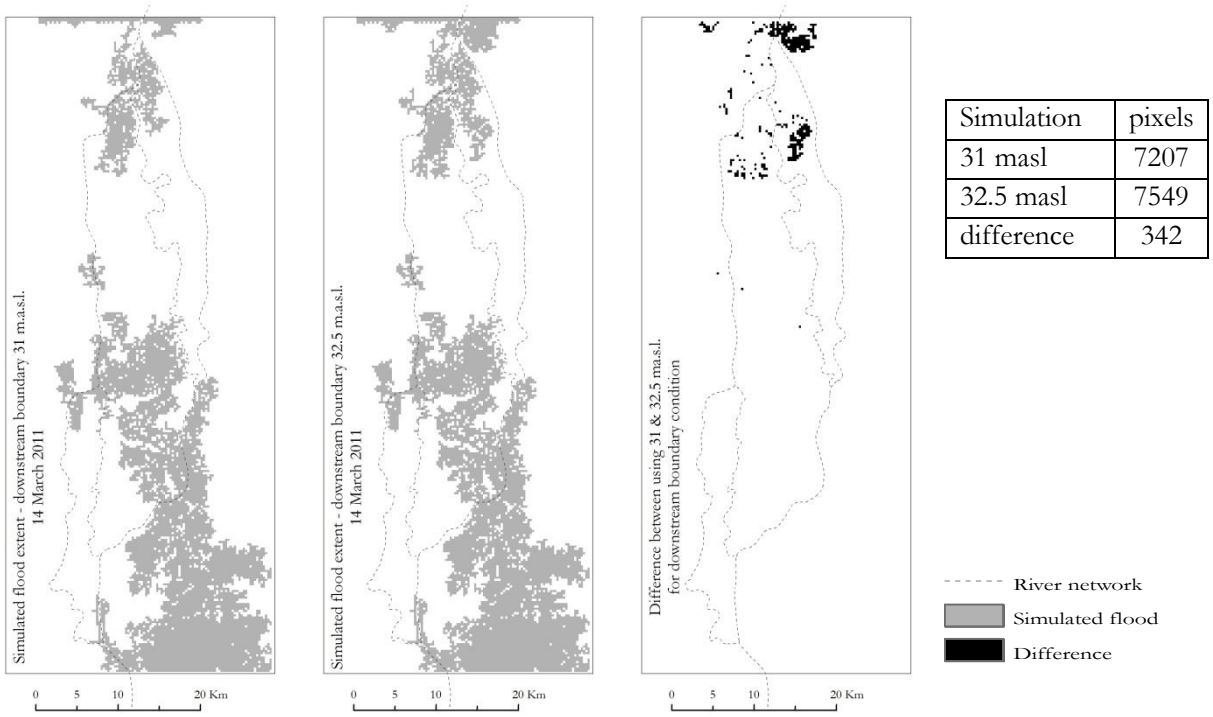

Simulation	pixels
31 masl	7207
32.5 masl	7549
difference	342

Figure 38. Contrasting flood simulations resulting from different downstream boundary conditions.

Having observed the effect of the different settings of surface roughness and boundary conditions on the simulated flood extents, it is also worthwhile to assess the effects on overland flow at different locations. Seven check point stations were defined along the southern portion of the floodplain to record simulated overland flow (Figure 39).

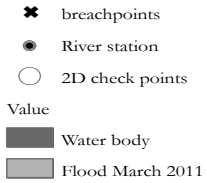

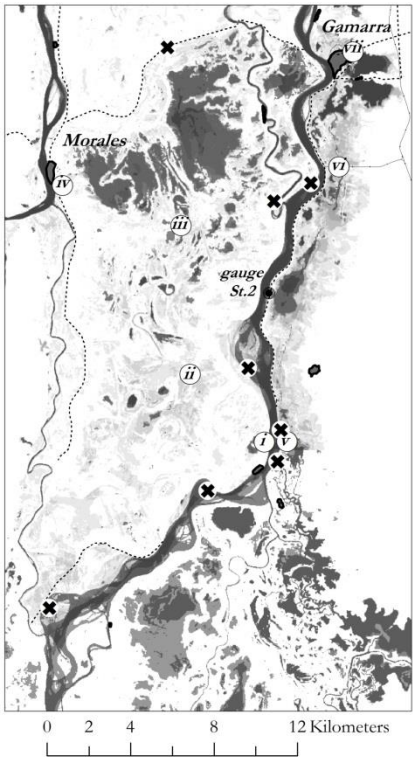

Figure 39. 2D check point stations for the final simulations.

The plots were prepared from three simulated cases (Figure 40); downstream boundary set at 32.5 m.a.s.l. and 31 m.a.s.l. with the same distributed surface roughness. With an additional case with downstream boundary at 31 m.a.s.l. and homogeneous surface roughness of 0.035. The first check point was set in an observed breach point, where also the river flow was overtopping.

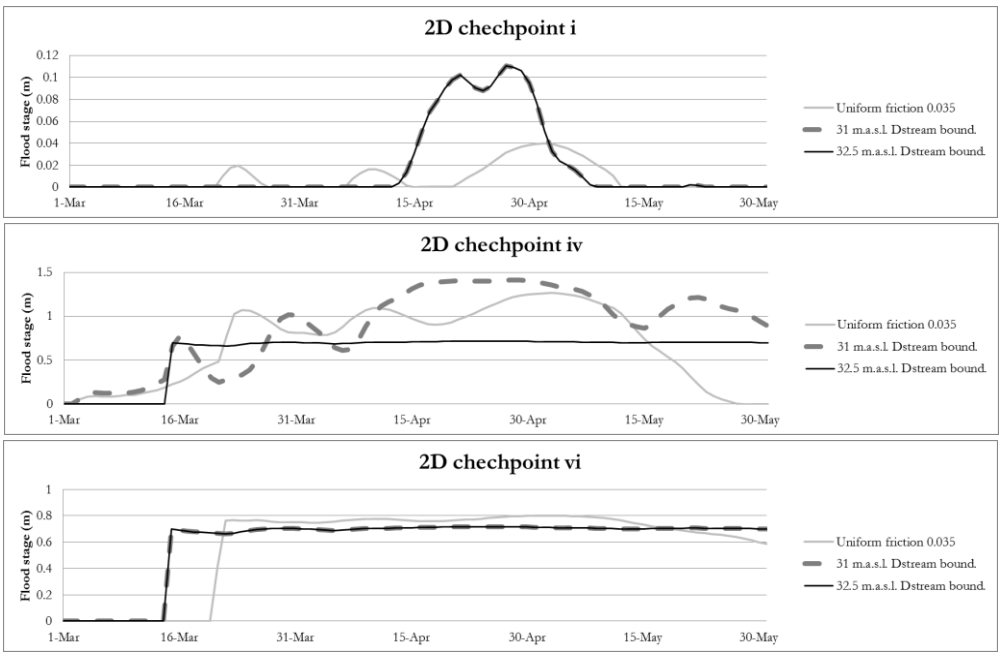

Figure 40. 2011 Simulated overland flow on check points i, iv and vi.

Plotting the simulated flood depth shows how the overbanking takes place and the effect of distributed and homogeneous surface roughness parameterization. Independent of the downstream boundary with distributed friction gives a more realistic result at this point with one wave in agreement to the flood event. A homogeneous friction value, does not induce much overbanking at this location besides the river bank. For the check point iv, located besides the town of Morales, the downstream boundary condition of 31 and 32.5 m.a.s.l. does have an effect on the simulated overland flow and flooding at these location. This location can receive flood waters from different directions, what creates such different patterns. Check point vi is located south of Gamarra town, where the railroad crosses the floodplain, and there again downstream boundary conditions do not have an effect and surface roughness has less effect, due to the morphology of that flooding area, which funnels water between the eastern terrace and the right bank of the main river. As the satellite images reveal, this zone is frequently flooded due to its morphology and further constrain by dikes and structures, representing a subsystem within the study area, being controlled by the boundary condition the southern wetland complex defines.

Spatial resolution of 90 vs. 270 meters per pixel

The result on using different spatial resolutions can be observed in the following Figure (Figure 41). From a total number of pixels simulated (17832), 72% of them coincide for both resolutions. 16% of total pixels just were flooded using the 90x90 meter/pixel resolution, while 12% was only flooded using the 270x270 meter/pixel resolution.

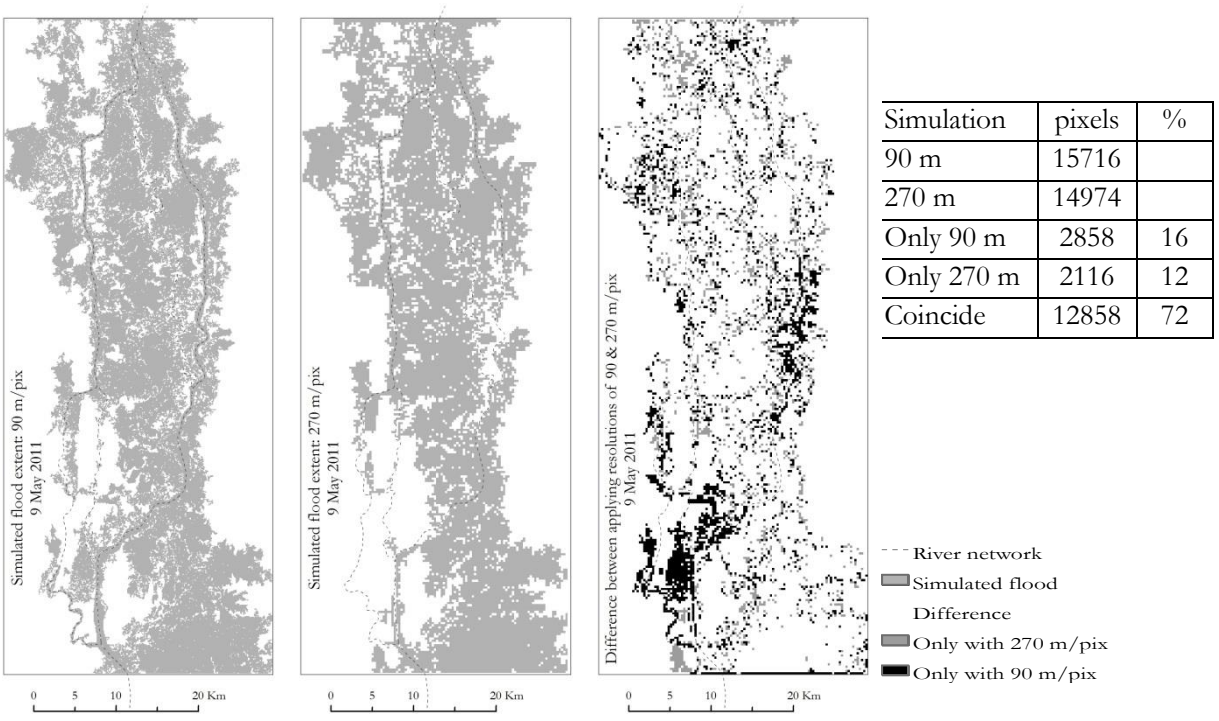

Simulation	pixels	%
90 m	15716	
270 m	14974	
Only 90 m	2858	16
Only 270 m	2116	12
Coincide	12858	72

Figure 41. Contrasting flood simulations resulting from different grid spatial resolutions.

2005 flood event

For the flood extent of December of 2005 (Figure 42), a flood extent was visible on the second day of the month. Comparing the classified flood extent with the simulated one, coincide in 30% of the total pixels (16194). 62% is only simulated and 8% of the total pixels is only classified or observed flood. The general pattern in they occupy is similar. The differences rely on several reasons; the flood classification misses to represent pixels that contain floating vegetation or standing bushes or trees above the flood. In the other hand the Landsat ETM contains some linear gaps which reduce the number of pixels in the count. The simulation misses to represent the lower left boundary where the second branch diverts from the main river.

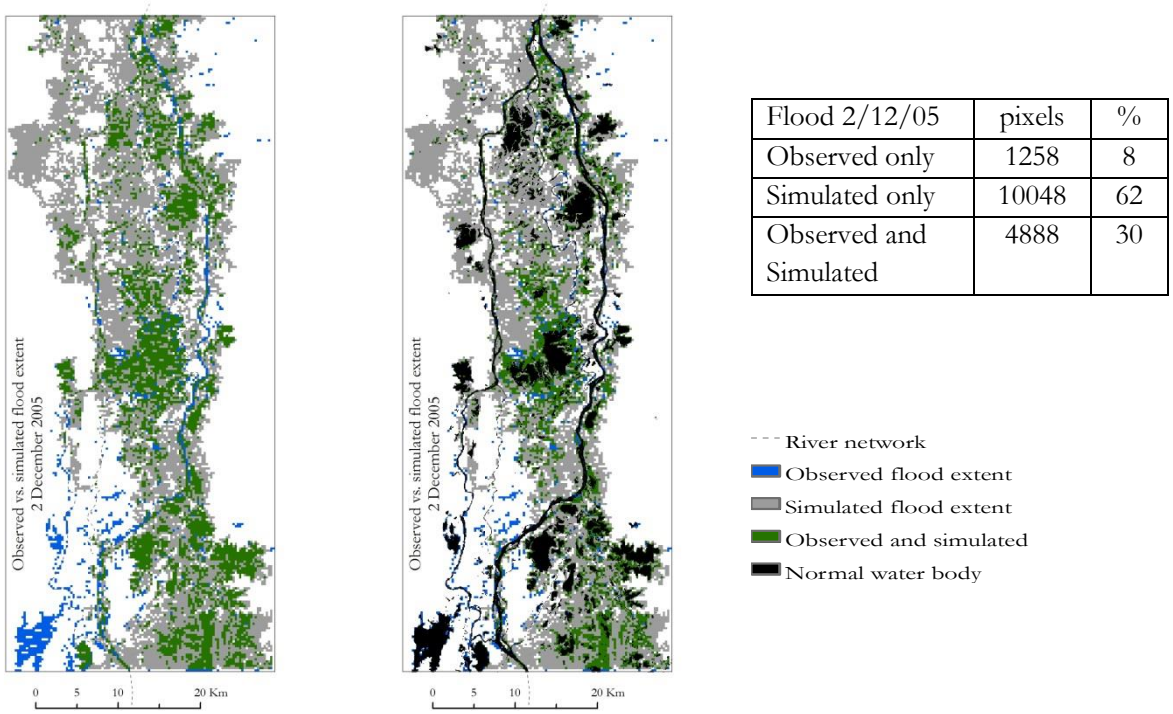

Flood 2/12/05	pixels	%
Observed only	1258	8
Simulated only	10048	62
Observed and Simulated	4888	30

Figure 42. Contrasting flood simulation and observed flood extent for December 2 2005.

2011 flood event

For the flood of May 2011 (Figure 43), a flood extent was visible on the ninth day of the month. This simulation was performed on 90x90 meter/pixel resolution. Comparing the interpreted flood extent with the simulated one coincides in 65% of the total pixels (193360). 4% is only simulated and 31% of the total pixels correspond only to the interpreted or observed flood. Due to the mapping method, visual interpretation does not capture all the pixels that contain mixed vegetation, the difference is made and the boundaries of the flood are drawn. Only some small areas in the floodplain showed indications that they did not flood.

As well as the simulation on 270x270 meter/pixel, the model does not reproduce the flooding pattern observed in the satellite imagery for the second branch, after diverting from the main river. Simulations also overestimate flooding along a wetland area on the north western side. Areas seen in blue, show the locations where the simulations did not present any flood, but are mapped as such.

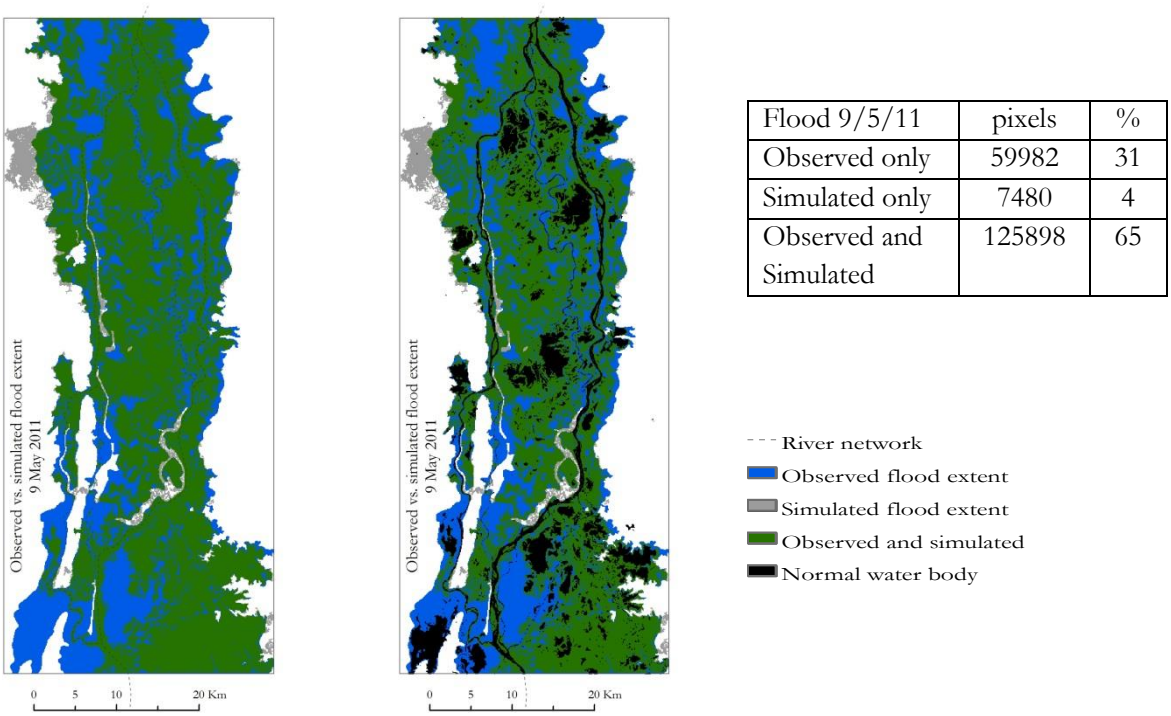

Flood 9/5/11	pixels	%
Observed only	59982	31
Simulated only	7480	4
Observed and Simulated	125898	65

Figure 43. Contrasting flood simulation and observed flood extent for May 9 2011.

An interesting and expected result from the simulations was the fact that the main river banks cannot hold the inflow from the south eastern (Lebrija) wetland and the floodplain at the right of the river has to be maintained as a buffer area in land management practices. Dikes have been constructed trying to prevent the water from coming inside that stretch but have failed. Designs have to go forward with a flood buffering concept for the area.

6. CONCLUSIONS & RECOMENDATIONS

6.1. Conclusions

The Magdalena River floodplain has historically been affected by interventions and is frequently subjected to flooding from high flows in the river. Confronting necessary development and grow in the floodplain with natural and hydrological requirements, is an urgent matter to take into account for land management and planning. Hydrodynamic 1D2D SOBEK flood model in combination with remote sensing and GIS offers valuable tools for flood assessments in the study area. Due to the lack of data remote sensing is a valuable alternative to base the flood model input requirements on. This model was made by testing different setups and performing evaluations on different parameter sets and resulting flood extents.

To achieve an initial representation, work in was done to obtain the required inputs for the 1D2D hydrodynamic model. Elevation was based on the CGIAR SRTM DEM and presented certain level of uncertainty that makes its use almost bearable. The elevation data can represent the general terrain of the floodplain, but need field survey to include the river cross section. Lacking river descriptions, a model cross section was used to describe the river bed and banks. The river bank interpolated elevations replaced the river surface elevation of the CGIAR product. Inaccurate simulated flood recession can be attributed to bank misrepresentation, causing increased water storage. Calculation grids were prepared on pixels of 270x270 and 90x90 meters. The resolution on 90 meters gave more sound results with considerable computing requirement.

River network description was successfully derived from Landsat imagery. Minor drainage network and water bodies need to be included for a more realistic representation of the study area. Flood and land cover maps were also produced as input and calibration sets. Pixel classification generally underestimates flood extent as many mixed pixels were missed, while by visual interpretation, overestimate of the flood extent was done as smaller dry areas within the flood matrix could have been missed. Tall or thick vegetation over a flooded terrain is also confused by both methods.

Upstream boundary conditions were set with the estimated discharge (at Station A) by IDEAM. These observations are based on daily river stage, which are calculated into discharge. The total series evidenced calibration issues, additionally observing the river widths at the station locations with Landsat images, it is concluded that this might partially be due to the changing morphology. High river flow was analysed and dates were selected to detect flooding and reproduce with simulations MODIS high resolution reflectance imagery is an important source of data regarding surface water extent detection for this study area.

Assessment of the river flow simulations was done on the location of two IDEAM gauge stations which had observed stage and estimated discharge daily series. The 1D model can reproduce rather well the observed series, but when coupling the 2D overland flow SOBEK module, the river flows become affected. When overbanking happens, downstream the peaks are greatly reduced. To assess the difference on the simulated flood extents with different parameter sets, several runs were done as means of parameter sensitivity tests.

An acceptable downstream boundary condition was defined at 31 m.a.s.l. Upstream boundary conditions that led to flooding were around 6500 m^3/s. For the 1D channel a Manning friction value of 0.25 is taken as acceptable, after performing a sensitivity analysis by increasing the friction and observing the time lag it induced on the peaks. The objective was to achieve 1 day difference between a peak upstream and

downstream as detected in the river gauges. Based on gauge observations the river flow diversion of 70% for the main river and 30% for the second branch is defined as acceptable. Further calibration of the model river section was made with the objective to reproduce the stage discharge relation on the main and second branch. By simulating steady state inflow boundary conditions the simulated stage discharge curve was constructed and selected the cross section set that could reproduce the observed pattern for final simulations.

270 meters is not an adequate resolution to perform 2D flood simulations, but still reflects some general flooding behaviour considered correct. 90 meter pixel improves on the detail, but still has errors similar to the coarse resolution. Indicating that the representation of the river and floodplain draining network is not well described. It is mainly due to the low capacity to describe the river and minor drainage network, including embankments and protection works along the river banks. Not only high water inflow determines a flood event. The spatial expression of a flood depends on a complex relation of factors that are not represented by the current model schematization. Simulated and observed flood extents were similar from 35% to 65%, for the events of December 2005 and May 2011. The mapping method has an effect on these figures.

The present model is considered preliminary and still in construction, due to the fact that important data is lacking on geometry and terrain aspects which govern overall performance. Important inflow points or additional boundary conditions upstream also have to be quantified. Downstream boundary conditions should also be investigated to have a more accurate representation of the system's properties. Temporal resolution on river flow measurements should be implemented, at least on short surveys different flow conditions and to complement river cross sections. Once the model is calibrated and produces accepted results, applications for land management and even aquatic ecosystems can be implemented.

6.2. Recomendations

Representing a starting point, this research gives way to identify data quality issues on required inputs for hydrodynamic modelling in large river floodplains in Colombia. Considerable field surveys and monitoring have to be done on different lines of work to meet input requirements. Elevation correction and link between the gauges of the monitoring system and datum, detailed elevation representation on infrastructure, protection works and river banks as well as drainage network has to be done. Flood monitoring stations should be implemented for this flood prone area. 1D2D hydrodynamic modelling should have permanent feedback with field data and decision makers.

Modelling environmental processes and aquatic systems is basic for land planning and management in floodplains. In consequence setting up and running such dynamic models in scares data contexts, gives the first steps in designing survey and monitoring campaigns for a permanent modelling, field work and decision making in the context of land management. At the same time data access has to be increased, opening official data sets online, as available data sets open the possibility to analyse them.

Not only changing climate and recurrent extremes pose challenge and uncertainty on modelling & scenario applications, changing morphology is an important factor to consider, due to natural and human induced changes in the river and flooding plain. It is important to engage efforts in improving the monitoring system and the application of collected data in hydrodynamic flood modelling for land management in the Magdalena River floodplain.

LIST OF REFERENCES

Alfonso Segura, J. L. (2010). *Optimisation of Monitoring Networks for Water Systems. Information theory, value of information and public participation.* (Vol. PhD Thesis). Delft: IHE UNESCO.

Amador Berrío, F. E. (2013). *Master Programme Development of a Methodology for Producing Probabilistic Flood Maps of River-Wetland Systems : Case Study of Magdalena River , Colombia Flood Maps of River-Wetland Systems : Case Study of*. UNESCO-IHE.

Arcement, Jr., G. J., Schneider, V. R., & USGS. (1989). Guide for Selecting Manning ' s Roughness Coefficients for Natural Channels and Flood Plains United States Geological Survey Water-supply Paper 2339. *Paper 2339*. http://doi.org/Report No. FHWA-TS-84-204

Bates, P. D., & De Roo, a. P. J. (2000). A simple raster-based model for flood inundation simulation. *Journal of Hydrology*, *236*(1-2), 54–77. http://doi.org/10.1016/S0022-1694(00)00278-X

CI Conservacion Internacional. (2015). index @ www.tremarctoscolombia.org. Retrieved August 8, 2015, from http://www.tremarctoscolombia.org/

Costabile, P., & Macchione, F. (2015). Enhancing river model set-up for 2-D dynamic flood modelling. *Environmental Modelling & Software*, *67*, 89–107. http://doi.org/10.1016/j.envsoft.2015.01.009

Da Silva, J. S., Seyler, F., Calmant, S., Rotunno Filho, O. C., Roux, E., Araújo, A. A. M., & Guyot, J. L. (2012). Water level dynamics of Amazon wetlands at the watershed scale by satellite altimetry. *International Journal of Remote Sensing*, *33*(11), 3323–3353. http://doi.org/10.1080/01431161.2010.531914

Deltares. (2014). SOBEK user manual; Hydrodynamic, rainfall runoff and real time control, (1).

El-Shaarawi, A. H., & Piegorsch, W. W. (Eds.). (2002). *Encyclopedia of Environmetrics* (Volume 2). John Wiley & Sons.

Foro Nacional Ambiental. (2015). Foro Nacional Ambiental - Rio Magdalena, impactos socio economicos. Retrieved January 10, 2016, from http://www.foronacionalambiental.org.co/actividades/detalle/foro-publico-para-donde-va-el-rio-magdalena-riesgos-sociales-ambientales-y-economicos-del-proyecto-de-navegabilidad-2/

Frazier, P. S., & Page, K. J. (2000). Water Body Detection and Delineation with Landsat TM Data, *66*(12), 1461–1467.

Gallant, J., & Read, A. (2009). Enhancing the SRTM data for Australia. *Proceedings of Geomorphometry. 31 Aug/2 Sept. Zurich, Switzerland.*, (Figure 1), 149–154. Retrieved from http://www.geomorphometry.org/sites/default/files/gallantb2009geomorphometry.pdf

Garcia, R. P. E. (2015). Hydraulic Design Manual. Retrieved January 5, 2016, from http://onlinemanuals.txdot.gov/txdotmanuals/hyd/manual_introduction.htm

Gieske, A., W W, A., H a, G., T H, A., & Rientjes, T. (2008). Non-Linear Parameterization of Lake Tana ' S Flow System. *Proceedings of the Workhop on Hydrology and Ecology of the Nile River Basin under Extreme Conditions : Addis Ababa, Ethiopia, June 16-19, 2008. Editor W. Abtew, A.M. Melesse. Miami : Florida International University, 2008.*, 127–144. Retrieved from ISBN 978-1-4276-3150-3

Gilles, D., & Moore, M. (2010). Review of Hydraulic Flood Modeling Software used in Belgium , The Netherlands , and The United Kingdom. *Europe*.

Goosen, D. (1961). A study of geomorphology and soils in the middle Magdalena Valley, Colombia. ITC Publications Series B. Photo-interpretation. Vol. B9. Delft.

Gorokhovich, Y., & Voustianiouk, a. (2006). Accuracy assessment of the processed SRTM-based elevation data by CGIAR using field data from USA and Thailand and its relation to the terrain characteristics. *Remote Sensing of Environment*, *104*(4), 409–415. http://doi.org/10.1016/j.rse.2006.05.012

Hidayat, H., Hoekman, D. H., Vissers, M. a. M., & Hoitink, a. J. F. (2011). Combining ALOS-PALSAR imagery with field water level measurements for flood mapping of a tropical floodplain. *International Symposium on Lidar and Radar Mapping 2011: Technologies and Applications*, *8286*, 82861X. http://doi.org/10.1117/12.912735

Ho, L. T. K., Umitsu, M., & Yamaguchi, Y. (2010). Flood hazard mapping by satellite images and SRTM DEM in the Vu Gia-Thu Bon alluvial plain, Central Vietnam. *International Archives of the Photogrammetry, Remote Sensing and Spatial Information Science*, *XXXVIII*(part8), 275–280.

Hoyos, N. (2013). Impact of the 2010-2011 La Niña phenomenon in Colombia, South America: The human toll of an extreme weather event. *Applied Geography*, *39*(September 2011), 16–25. http://doi.org/10.1016/j.apgeog.2012.11.018

Huang, C., Chen, Y., & Wu, J. (2014). Mapping spatio-temporal flood inundation dynamics at large river basin scale using time-series flow data and MODIS imagery. *International Journal of Applied Earth Observation and Geoinformation*, *26*, 350–362. http://doi.org/10.1016/j.jag.2013.09.002

Huthoff, F., Remo, J. W. F., & Pinter, N. (2013). Improving flood preparedness using hydrodynamic levee-breach and inundation modelling: Middle Mississippi River, USA. *Journal of Flood Risk Management*, (Revision 1), n/a–n/a. http://doi.org/10.1111/jfr3.12066

Ipcc, I. P. O. C. C. (2007). Climate Change 2007: The Physical Science Basis. *Energy Environment*, *18*(3), 433–440. http://doi.org/10.1080/03736245.2010.480842

Jarvis, A., Rubiano, J., Nelson, A., Farrow, A., & Mulligan, M. (2004). Practical use of SRTM data in the tropics – Comparisons with digital elevation models generated from cartographic data. *Tropical Agriculture*, *198*, 32. Retrieved from http://citeseerx.ist.psu.edu/viewdoc/download?doi=10.1.1.110.3805&rep=rep1&type=pdf

Joyce, K. E., Belliss, S. E., Samsonov, S. V., McNeill, S. J., & Glassey, P. J. (2009). A review of the status of satellite remote sensing and image processing techniques for mapping natural hazards and disasters. *Progress in Physical Geography*, *33*(2), 183–207. http://doi.org/10.1177/0309133309339563

Kanoua, W., & Merkel, B. J. (2015). Modification of a digital elevation model (DEM) in a flat topographic area with respect to manmade features. *Geosciences Journal*. http://doi.org/10.1007/s12303-015-0020-7

Karim, F., Petheram, C., Marvanek, S., Ticehurst, C., Wallace, J., Gouweleeuw, B., … Anderssen, R. S. (2011). The use of hydrodynamic modelling and remote sensing to estimate floodplain inundation and flood discharge in a large tropical catchment. *19th International Congress on Modelling and Simulation (Modsim2011)*, (December), 3796–3802.

Kellndorfer, J., Walker, W., Pierce, L., Dobson, C., Fites, J. A., Hunsaker, C., … Clutter, M. (2004). Vegetation height estimation from Shuttle Radar Topography Mission and National Elevation Datasets. *Remote Sensing of Environment*, *93*(3), 339–358. http://doi.org/10.1016/j.rse.2004.07.017

Kolecka, N., & Kozak, J. (2014). Assessment of the Accuracy of SRTM C- and X-Band High Mountain Elevation Data: A Case Study of the Polish Tatra Mountains. *Pure and Applied Geophysics*, *171*(6), 897–912. http://doi.org/10.1007/s00024-013-0695-5

Manyifika, M. (2015). Diagnostic assessment on urban floods using satellite data and hydrologic models in Kigali, Rwanda. *ITC Thesis*. Retrieved from http://www.itc.nl/library/papers_2015/msc/wrem/manyifika.pdf

Melrose, R. T., Kingsford, R. T., & Milne, a. K. (2012). Using radar to detect flooding in arid wetlands and rivers. *International Geoscience and Remote Sensing Symposium (IGARSS)*, 5242–5245. http://doi.org/10.1109/IGARSS.2012.6352427

Merkuryeva, G., Merkuryev, Y., Sokolov, B. V., Potryasaev, S., Zelentsov, V. a., & Lektauers, A. (2014). Advanced river flood monitoring, modelling and forecasting. *Journal of Computational Science*. http://doi.org/10.1016/j.jocs.2014.10.004

Mosquera-Machado, S., & Ahmad, S. (2007). Flood hazard assessment of Atrato River in Colombia. *Water Resources Management*, *21*(3), 591–609. http://doi.org/10.1007/s11269-006-9032-4

Nash, E., & Sutcliffe, V. (1970). River flow forecasting through conceptual models. Part 1A discussion of principles. *Journal of Hydrology*, *10*, 282–290.

Oswalt, S. N., & King, S. L. (2005). Channelization and floodplain forests: Impacts of accelerated sedimentation and valley plug formation on floodplain forests of the Middle Fork Forked Deer River, Tennessee, USA. *Forest Ecology and Management*, *215*(1-3), 69–83. http://doi.org/10.1016/j.foreco.2005.05.004

Poole, G. C., Stanford, J. A., Frissell, C. A., & Running, S. W. (2002). Three-dimensional mapping of geomorphic controls on flood-plain hydrology and connectivity from aerial photos, *48*, 329–347.

Poretti, I., & De Amicis, M. (2011). An approach for flood hazard modelling and mapping in the medium Valtellina. *Natural Hazards and Earth System Science*, *11*(4), 1141–1151. http://doi.org/10.5194/nhess-11-1141-2011

Restrepo, J. D., & Kjerfve, B. (2000). Magdalena river: Interannual variability (1975-1995) and revised water discharge and sediment load estimates. *Journal of Hydrology*, *235*(1-2), 137–149. http://doi.org/10.1016/S0022-1694(00)00269-9

Reuter, H. I., Nelson, a., & Jarvis, a. (2007). *An evaluation of void-filling interpolation methods for SRTM data*. *International Journal of Geographical Information Science* (Vol. 21). http://doi.org/10.1080/13658810601169899

Robinson, J. B., Hazell, W. F., Young, W. S., & USGS. (1998). Effects of August 1995 and July 1997 Storms in the City of Charlotte and Mecklenburg County, North Carolina. Retrieved January 10, 2016, from http://pubs.usgs.gov/fs/FS-036-98/text/what.html

Royal Haskoning. (2015). Royal Haskoning, flood contract in Colombia. Retrieved October 1, 2016, from http://www.royalhaskoningdhv.com/en-gb/news-room/news/20130806pr-major-flood-control-contract-colombia/597

Royal Haskoning. (2016). Royal Haskoning, floods in Colombia. Retrieved from http://www.royalhaskoningdhv.com/en-gb/news-room/news/20130806pr-major-flood-control-contract-colombia/597

Rudorff, C. M., Melack, J. M., & Bates, P. D. (2014). Flooding dynamics on the lower Amazon floodplain: 1. Hydraulic controls on water elevation, inundation extent, and river-floodplain discharge. *Water Resources Research*, *50*(1), 619–634. http://doi.org/10.1002/2013WR014091

Sun, G., Ranson, K. J., Kharuk, V. I., & Kovacs, K. (2003). Validation of surface height from shuttle radar topography mission using shuttle laser altimeter. *Remote Sensing of Environment*, *88*(4), 401–411. http://doi.org/10.1016/j.rse.2003.09.001

Syvitski, J. P. M., Overeem, I., Brakenridge, G. R., & Hannon, M. (2012). Floods, floodplains, delta plains - A satellite imaging approach. *Sedimentary Geology*, *267-268*, 1–14. http://doi.org/10.1016/j.sedgeo.2012.05.014

Tarekegn, T. H., Haile, A. T., Rientjes, T., Reggiani, P., & Alkema, D. (2010). Assessment of an ASTER-generated DEM for 2D hydrodynamic flood modeling. *International Journal of Applied Earth Observation and Geoinformation*, *12*(6), 457–465. http://doi.org/10.1016/j.jag.2010.05.007

Te Linde, a. H., Aerts, J. C. J. H., & Kwadijk, J. C. J. (2010). Effectiveness of flood management measures on peak discharges in the Rhine basin under climate change. *Journal of Flood Risk Management*, *3*(4), 248–269. http://doi.org/10.1111/j.1753-318X.2010.01076.x

Teegavarapu, R. S. V. &, & UNESCO. (2012). *Floods in a changing climate. Extreme precipitation*. Cambridge University Press.

TNC The Nature Conservancy. (2014). floodplains-management @ www.nature.org. Retrieved August 8, 2015, from http://www.nature.org/ourinitiatives/regions/southamerica/colombia/floodplains-management.xml

UNESCO. (2015). Pre-Hispanic Hydraulic System of the San Jorge River - UNESCO World Heritage Centre. Retrieved from http://whc.unesco.org/en/tentativelists/5764/

Vogel, R. M., Yaindl, C., & Walter, M. (2011). Nonstationarity: Flood magnification and recurrence reduction factors in the united states. *Journal of the American Water Resources Association*, *47*(3), 464–474. http://doi.org/10.1111/j.1752-1688.2011.00541.x

Vorogushyn, S., Merz, B., Lindenschmidt, K. E., & Apel, H. (2010). A new methodology for flood hazard assessment considering dike breaches. *Water Resources Research*, *46*(8), 1–17. http://doi.org/10.1029/2009WR008475

Wolman, B. M. G., & Leopold, L. B. (1957). River Flood Plains : Some Observations On Their Formation. *Distribution*, *282-C*, 87–107. Retrieved from http://www.getcited.org/pub/102041013

ANNEXES

1. Historic river stages, El Heraldo.com, based on IDEAM.

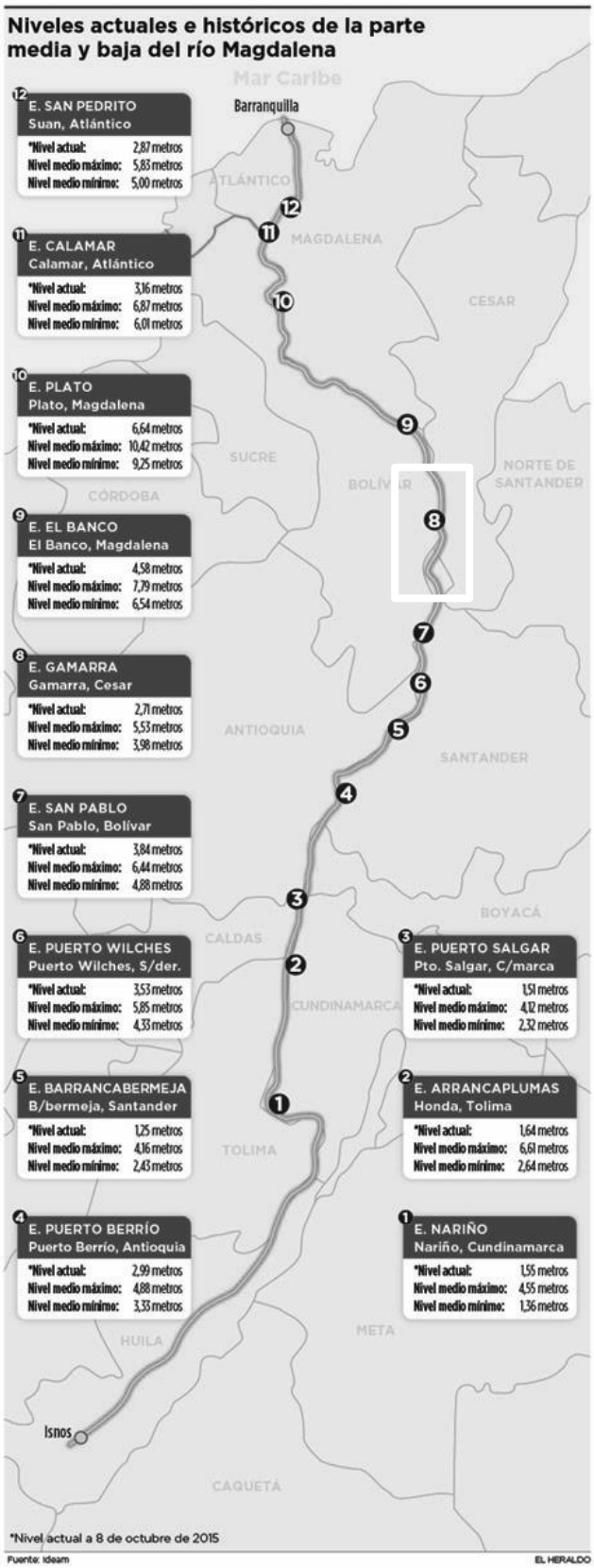

2. Elevation variation for homogeneous vegetation patches results.

grass					trees					sandy island					bare/sand				
path	elevation	elev step	npix	percpix	patch		elev step	npix	percpix	patch	elevation	elev step	npix	percpix	patch	elevation	elev step	npix	percpix
1	37	0	1	0.6	1	48	0	1	16.7	1	38	0	3	50.0	1	37	0	2	12.5
1	38	1	12	7.5	1	49	1	1	16.7	1	39	1	1	16.7	1	38	1	2	12.5
1	39	2	29	18.2	1	50	2	2	33.3	1	40	2	2	33.3	1	39	2	1	6.3
1	40	3	45	28.3	1	51	3	1	16.7				6		1	40	3	5	31.3
1	41	4	39	24.5	1	52	4	1	16.7						1	41	4	3	18.8
1	42	5	22	13.8				6		2	38	0	4	57.1	1	42	5	1	6.3
1	43	6	7	4.4						2	39	1	3	42.9	1	43	6	2	12.5
1	44	7	4	2.5	2	44	0	9	3.4				7					16	
			159		2	45	1	26	9.8										
					2	46	2	24	9.1	3	39	0	5	29.4	2	35	0	1	4.8
2	34	0	2	1.7	2	47	3	41	15.5	3	41	1	1	5.9	2	36	1	2	9.5
2	35	1	1	0.8	2	48	4	54	20.5	3	42	2	1	5.9	2	37	2	4	19.0
2	36	2	5	4.2	2	49	5	42	15.9	3	43	3	1	5.9	2	38	3	6	28.6
2	37	3	13	10.9	2	50	6	24	9.1	4	42	4	3	17.6	2	39	4	6	28.6
2	38	4	32	26.9	2	51	7	14	5.3	4	43	5	6	35.3	2	40	5	2	9.5
2	39	5	18	15.1	2	52	8	9	3.4				17					21	
2	40	6	26	21.8	2	53	9	9	3.4										
2	41	7	14	11.8	2	54	10	5	1.9	4	44	0	10	83.3	3	33	0	1	2.1
2	42	8	6	5.0	2	55	11	4	1.5	4	45	1	2	16.7	3	34	1	1	2.1
2	43	9	2	1.7	2	56	12	3	1.1				12		3	35	2	6	12.5
			119					264							3	36	3	5	10.4
										5	42	0	1	9.1	3	37	4	8	16.7
3	35	0	1	1.4	3	46	0	1	3.1	5	43	1	3	27.3	3	38	5	12	25.0
3	36	1	5	7.0	3	47	1	3	9.4	5	44	2	3	27.3	3	39	6	8	16.7
3	37	2	5	7.0	3	48	2	2	6.3	5	45	3	3	27.3	3	40	7	6	12.5
3	38	3	9	12.7	3	49	3	2	6.3	5	47	4	1	9.1	3	41	8	1	2.1
3	39	4	16	22.5	3	50	4	5	15.6				11					48	
3	40	5	22	31.0	3	51	5	4	12.5										
3	41	6	8	11.3	3	52	6	6	18.8	6	44	0	2	11.1					
3	42	7	2	2.8	3	53	7	4	12.5	6	45	1	3	16.7	rice				
3	43	8	3	4.2	3	54	8	3	9.4	6	46	2	5	27.8	patch	elevation	elev step	npix	percpix
			71		3	55	9	2	6.3	6	47	3	5	27.8					
								32		6	48	4	3	16.7	1	36	0	1	5.0
4	36	0	2	3.3									18		1	37	1	3	15.0
4	37	1	15	24.6	4	44	0	2	4.2						1	38	2	9	45.0
4	38	2	12	19.7	4	45	1	9	18.8	7	43	0	2	9.5	1	39	3	4	20.0
4	39	3	17	27.9	4	46	2	8	16.7	7	44	1	2	9.5	1	40	4	3	15.0
4	40	4	10	16.4	4	47	3	5	10.4	7	45	2	10	47.6				20	
4	41	5	4	6.6	4	48	4	6	12.5	7	46	3	3	14.3					
4	42	6	1	1.6	4	49	5	6	12.5	7	47	4	2	9.5	2	38	0	1	12.5
			61		4	50	6	5	10.4	7	48	5	1	4.8	2	41	1	3	37.5
					4	51	7	5	10.4	7	51	6	1	4.8	2	42	2	3	37.5
5	31	0	1	1.3	4	52	8	1	2.1				21		2	43	3	1	12.5
5	32	1	1	1.3	4	53	9	1	2.1									8	
5	33	2	10	13.0				48		8	46	0	4	25.0					
5	34	3	10	13.0						8	47	1	1	6.3	3	39	0	1	6.7
5	35	4	22	28.6	5	44	0	1	5.3	8	48	2	2	12.5	3	40	1	5	33.3
5	36	5	20	26.0	5	45	1	2	10.5	9	45	3	3	18.8	3	41	2	6	40.0
5	37	6	10	13.0	5	46	2	4	21.1	9	46	4	4	25.0	3	42	3	3	20.0
5	38	7	3	3.9	5	47	3	6	31.6	9	48	5	1	6.3				15	
			77		5	48	4	4	21.1	9	49	6	1	6.3	tree grass now				
					5	49	5	1	5.3				16		patch	elevation	elev step	npix	
					5	50	6	1	5.3										
								19							1	37	0	2	
															1	38	1	2	
					6	36	0	1	3.3						1	39	2	1	
					6	37	1	8	42.1						1	40	3	3	
					6	38	2	10	52.6						1	41	4	7	
					6	39	3	6	31.6						1	42	5	11	
					6	40	4	4	21.1						1	43	6	17	
					6	41	5	1	5.3						1	44	7	21	
								30							1	45	8	31	
															1	46	9	30	
															1	47	10	16	
															1	48	11	9	
															1	49	12	1